6-30-1974

Optimal performance of equilibrium parametric pumps

Joseph A. Manganaro
New Jersey Institute of Technology

Recommended Citation

Manganaro, Joseph A., "Optimal performance of equilibrium parametric pumps" (1974). *Theses*. 2180.
https://digitalcommons.njit.edu/theses/2180

OPTIMAL PERFORMANCE OF EQUILIBRIUM PARAMETRIC PUMPS

BY

JOSEPH A. MANGANARO

A THESIS

PRESENTED IN PARTIAL FULFILLMENT OF

THE REQUIREMENTS FOR THE DEGREE

OF

MASTER OF SCIENCE IN CHEMICAL ENGINEERING

AT

NEWARK COLLEGE OF ENGINEERING

Newark, New Jersey

1974

ABSTRACT

An examination of the conditions required to obtain the optimal performance of semicontinuous and continuous parametric pumps, defined by the achieving of the maximum possible solute free product for a given column height, was undertaken. The model system sodium nitrate - water on an ion retardation resin adsorbate was employed. Equations defining maximum values of certain important parameters such as the bottom product flow rate and reservoir displacement rate were developed by extending previous theories of parametric pumping. Experimental runs were carried out using parameters whose values were both less than and greater than the maximum values predicted for optimal performance. It was found that for pumps operating with parameter values less than the limiting maximum values, complete removal of solute from the bottom of the column was obtained. Furthermore, for those pumps for which the parameter values were greater than the predicted maximum quantities only partial removal of solute was observed. The experimental results agreed quantitatively as well as qualitatively with the theory for almost all runs.

APPROVAL OF THESIS

OPTIMAL PERFORMANCE OF EQUILIBRIUM PARAMETRIC PUMPS

BY

JOSEPH A. MANGANARO

FOR

DEPARTMENT OF CHEMICAL ENGINEERING

BY

FACULTY COMMITTEE

APPROVED:

NEWARK, NEW JERSEY

JUNE, 1974

ACKNOWLEDGEMENTS

Sincere appreciation and gratitude are extended to Dr. H. T. Chen, whose advice and assistance were instrumental in making this investigation possible. Thanks is also extended to A. Zikri and W. Lin for their helpful advice with regard to experimental technique.

Parts of this research project have been presented at the A. C. S. National Meeting in Atlantic City, New Jersey, September, 1974.

TABLE OF CONTENTS

LIST OF FIGURES

LIST OF TABLES

INTRODUCTION

Parametric pumping is a separation process consisting of a solid phase adsorbent and a fluid phase containing two or more components. The extent to which a component will adsorb onto the solid is dependent upon the intensity of some chosen property under which the process is operated, such as temperature, pressure, or pH. If the direction of the fluid flow is changed periodically with the intensity of the operating property, a change in the concentration of components will occur along the flow path. Under certain operating conditions complete depletion of one or more components may occur at some point, thus separating them from those which remain.

In previous work (1) Chen and Hill, by extending the equilibrium theory of Pigford, Baker, and Blum (4), derived mathematical expressions for the performance of parametric pumps for continuous and semicontinuous modes of separation. They have found with experimental varification that depending upon the relative intensities of certain parameters, three distinct regions of separation exist for these modes. One region is characterized by the eventual and complete removal of solute at one product stream with a certain level of solute enrichment present at the other product stream. The other two regions are characterized by only partial removal of solute from one product stream with some solute enrichment at the other end.

Since in most cases complete or nearly complete removal of solute is desired, the operating parameters of the pump should be adjusted in such a way so as to insure operation in the proper region of separation. Because the set of possible combinations of such adjusted parameter values is virtually infinite, it is desired to limit these combinations to give only the best separations and yields with acceptable degrees of economic feasability. In order to do this a study of region boundary conditions is employed to find the limiting and maximum values of the important parameters. From here, the theory for the optimal performance of continuous and semicontinuous parametric pumps is developed and extended for multicomponent systems.

In this thesis thermal continuous and semicontinuous pumps with feed entering at the top are used for the investigation of optimal pump performance using the model system sodium nitrate - water on an ion retardation resin adsorbent. A comparison is made between the experimental data and the analytical formulations for both the operation and optimization of the pump. Emphasis is given on the operating conditions nessecary to achieve very high degrees of separation with maximum yields. Information in connection with such optimal values of operating parameters is essential for design or scale-up purposes.

The problem of nitrates in drinking water is one of increasing concern. Nitrate salts accumulate in surface and groundwater as a result of contamination by industrial or organic waste products and chemical fertilizers. The high nitrate drinking water which may result is especially harmful to infants, causing a blood disease known as methemoglobinemia. High concentrations of nitrates in lakes and streams can result in abnormal increases in vegitation which remove oxygen from the water, and can cause water discoloration and unpleasant odors. This nitrate problem creates a need for an effective and economical way of separating excess nitrates from water. Chemical neutralization, distillation, filtration, conventional ion exchange, and electromechanical processes are some of the methods being investigated (3). This paper presents one more possibility for solving this problem.

EXPERIMENTAL

A. Description of Equipment

The operation of both continuous and semicontinuous parametric pumps on the laboratory scale involved a jacketed pyrex glass column ninety centimeters in length and one centimeter in width which was packed with adsorbent particles. Top and bottom fluid reservoirs in the form of 50 cc glass syringes were operated by an infusion-withdrawal pump manufactured by Harvard apparatus. The feed reservoir, which was also a 50 cc glass syringe, was operated by an infusion pump only. All syringes were sealed with stopcock grease, and their contents were magnetically stirred to insure uniform concentration distribution within the reservoir. Solenoid valves were used to change the source of the fluid flow entering the jacket from the hot water bath to the cold water bath so that the desired column temperature corresponding to a specified flow direction was obtained. The top and bottom product flow rates were controlled with the use of micrometric capillary valves, and the products were collected in 10. ml graduated cylinders. All flow lines were made of 0.031 inch ID teflon tubing. (See figure 1.)

B. Experimental Procedure

At time zero the top and bottom reservoirs, the feed reservoir, and the void volume inside the adsorbent-filled

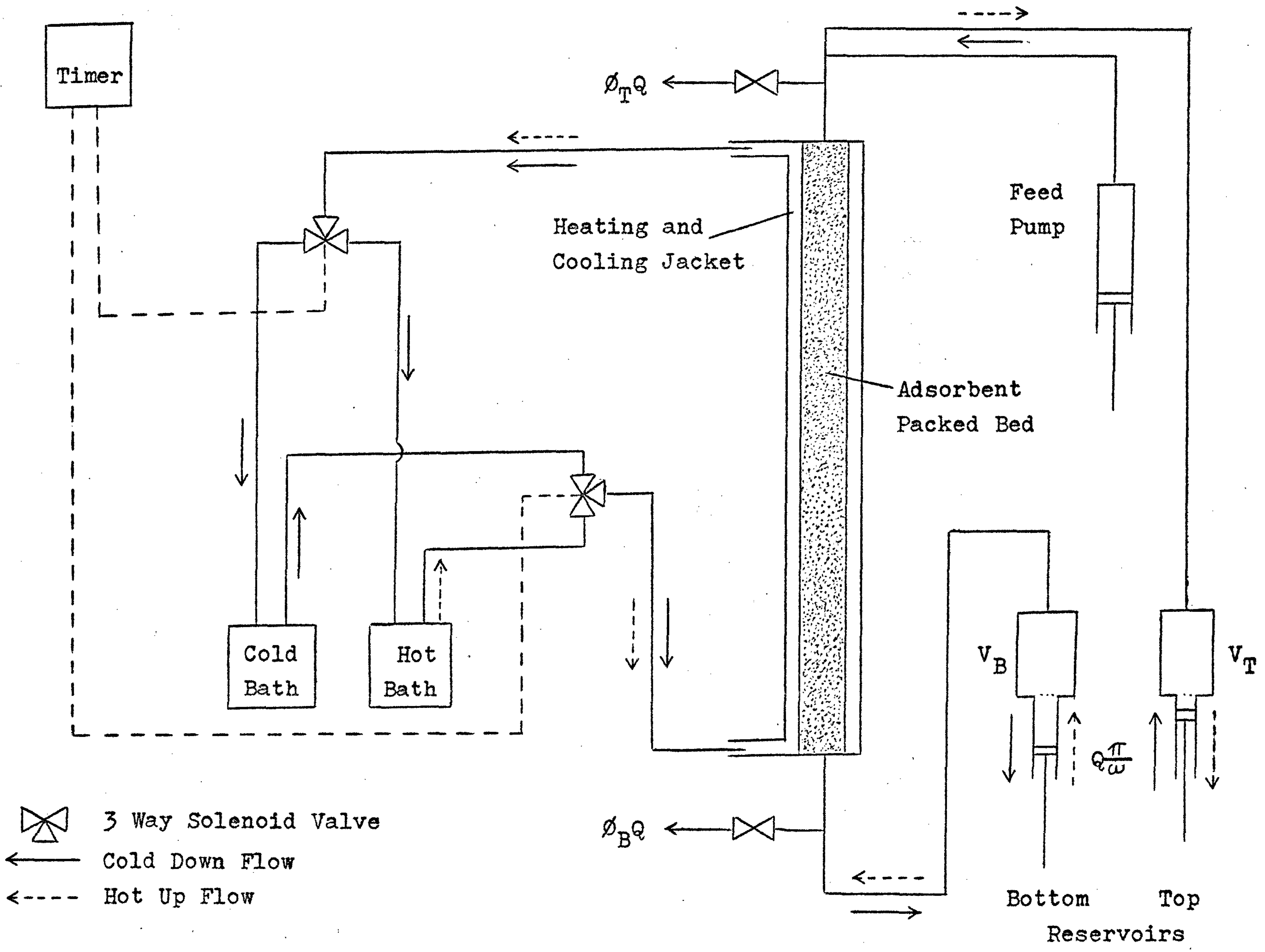
Timer
$\varnothing_T Q$
Heating and Cooling Jacket
Feed Pump
Adsorbent Packed Bed
Cold Bath
Hot Bath
V_B
V_T
$Q\frac{\pi}{\omega}$
$\varnothing_B Q$
Bottom
Top
Reservoirs
3 Way Solenoid Valve
Cold Down Flow
Hot Up Flow

Figure 1

column were filled with approximately 0.0250 molar sodium nitrate solution at room temperature. After all desired flow rates and dead volume settings were adjusted on the apparatus, pump operation was started with upflow from the bottom reservoir to the top reservoir occuring during the hot temperature period. In the case of the continuous pump, top and bottom products were collected at controlled rates with feed entering the top of the column at about 0.25 cc/min. . In the semicontinuous pump, however, no feed or product flow existed in the hot temperature upflow period. After twenty minutes the reciprocating action of the pump reversed the flow direction of the fluid, which now traveled from the top reservoir to the bottom reservoir. At this time the solenoid valves switched to cold temperature flow inside the jacket. During the cold period both semicontinuous and continuous pumps were fed with solution at the top, and products were collected. After another twenty minutes this cycle, consisting of both hot and cold temperature periods was repeated fifteen times.

C. Method of Product Concentration Measurement and Calibration

The top and bottom product samples collected during the cold half cycle for both types of pumps were diluted for the purposes of measuring their respective concentrations. In all cases 0.500 ml. of bottom product was pipetted into 50.0 ml. of distilled water. The dilution factor for the bottom product samples was thus, (50.0 + .500) divided by .500 or 101 (i. e., the concentration of bottom product was 101 times that of the measured, diluted sample). Similarly, 1.00 ml. of top product was pipetted into 50.0 ml. of water, resulting in a dilution factor of 51.0 .

The product concentrations were measured with the use of an electrolytic conductivity - resistivity bridge manufactured by Leeds and Northrup. Resistivity measurements were made at 25.0°C using a conductivity cell with a cell constant of 1.00 ± .01 . A calibration table of resistivity readings corresponding to sodium nitrate concentrations was made by measuring carefully prepared solutions of known concentration (table 1). If the resistivity is plotted against $NaNO_3$ concentration on normal cartesian coordinates the curve of figure 2 results. As figures 3 to 6 show, the resistivity was found to be a linear function of concentration on the log-log scale having a slope of -.959 and the equation,

$$\log(R) = -.959\log(y) + .962 \qquad (1)$$

where R is the resistivity in ohms and y is the sodium nitrate concentration in g-moles/liter. Solving for the risistivity as a function of concentration,

$$R = 9.161y^{-.959} \qquad (1a)$$

A workable expression for the $NaNO_3$ concentration as a function of resistivity resulting from eq. (1) is,

$$y = 10.07R^{-1.043} \tag{1b}$$

If eq. (1b) is multiplied by the respective dilution factors for the top and bottom product samples and divided by the feed concentration y_o, the dimensionless concentrations normalized by y_o which result are,

$$\frac{\langle y_{BP2} \rangle_n}{y_o} = \frac{1017R_{BP}^{-1.043}}{y_o} \tag{1c}$$

for the bottom product and

$$\frac{\langle y_{TP2} \rangle_n}{y_o} = \frac{513.5R_{TP}^{-1.043}}{y_o} \tag{1d}$$

for the top product, where n is the cycle number, TP2 and BP2 are the top and bottom product designations during downflow respectively, and $\langle \; \rangle$ refers to the average value over a cycle. Table 2 presents a list of all major experimental parameters for all of the runs carried out, and figures 9 to 12 along with tables 3 to 10 show the experimental results.

D. The Nature of the Adsorbent

The resin used for the adsorbent in this investigation was AG11A8 ion retardation resin produced by Bio-Rad Laboratories. This resin, which differs markedly from conventional deionization and ion exchange resins, has a unique structure consisting of adjacent anion and cation exchange sites. These sites attract mobile anions and cations and associate weakly with them. As a result, the resin adsorbs both anions and cations in equivalent amounts, and due to the neutrality of the resin, substances are recovered in a salt free, non-ionic state. This adsorbent is made of spherical polymer beads containing the paired anion and cation exchange sites. When the resin is free of adsorbed salts (self-adsorbed form), each group is the counter ion of the other form. The structure of the resin is shown by the following diagram:

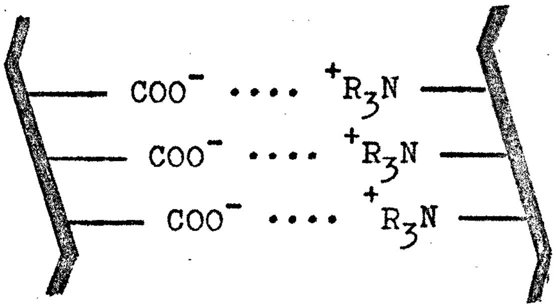

where the solid curved lines represent the organic polymer lattice. Inorganic ions are adsorbed with a mechanism differing from that of conventional ion exchange shown by the following:

$$\Bigg\}\mathrm{COOH} + \mathrm{Na}^{+} \longrightarrow \Bigg\}\mathrm{COONa} + \mathrm{H}^{+}$$

$$\Bigg\}\mathrm{NR_3OH} + \mathrm{NO_3}^{-} \longrightarrow \Bigg\}\mathrm{NR_3NO_3}^{-} + \mathrm{OH}^{-}$$

In the case of this resin, however,

$$\Bigg\}\mathrm{COO}^{-} \cdots\cdots {}^{+}\mathrm{R_3N}\Bigg\{ + \mathrm{NaNO_3} \longrightarrow \Bigg\}\mathrm{COONa}\quad \mathrm{NO_3R_3N}\Bigg\{$$

THEORY

The time it takes for fluid to flow in a particular direction at a certain temperature is called the half cycle time and is designated by the half cycle displacement distance π divided by the frequency of the cycle or π/ω. Flow to and from the reservoirs of all pumps during each half cycle is at the rate Q volume units per unit time so that the displacement volume is $Q\pi/\omega$. All pumps have dead volumes of size V_T and V_B volume units associated with the top and bottom reservoirs respectively. The feed flow rate is $(\phi_T + \phi_B)Q$, and the top and bottom flow rates are $\phi_T Q$ and $\phi_B Q$, where ϕ_T and ϕ_B are the ratios of top and bottom product flow rates P_T and P_B to the reservoir displacement rate Q.

Depending upon the relationships between the lengths of penetration distances of concentration waves during upflow and downflow with themselves and with the height of the column, one of three regions of separation might be encountered (see appendix, pg. 72). The only region characterized by complete, eventual removal of solute is region one; and it is established if $L_2 \leq L_1$ and h, where L_2 and L_1 are the penetration distances during downflow and upflow respectively, and h is the height of the column. For the continuous pump

$$L_1 = \frac{Q(1 - \phi_B)}{A\epsilon(1 + m_o)(1 - b)} \frac{\pi}{\omega} \tag{2}$$

and

$$L_2 = \frac{Q(1 + \phi_B)}{A\epsilon(1 + m_o)(1 + b)} \frac{\pi}{\omega} \tag{2a}$$

where A is the area normal to flow, ϵ is the fraction of the column occupied by void (fluid) volume, and m_o and b are equilibrium parameters. The quantity b is a measure of the extent of movement of solute between phases as a result of a change in column temperature and may be as small as zero for a system in which the equilibrium distribution is insensitive to temperature or as large as unity for which distribution is highly temperature sensitive. m_o is a quantity proportional to the thermal equilibrium constant at the mean temperature of the cycle (see appendix, pg. 69, for the development of eqs. (2) and (2a) and a further explanation of the equilibrium parameters involved).
Since, for operation in region one, $L_2 \leq L_1$,

$$\frac{Q(1 + \phi_B)}{A\epsilon(1 + m_o)(1 + b)} \frac{\pi}{\omega} \leq \frac{Q(1 - \phi_B)}{A\epsilon(1 + m_o)(1 - b)} \frac{\pi}{\omega}$$

or

$$\frac{1 + \phi_B}{1 + b} \leq \frac{1 - \phi_B}{1 - b}$$

which leads to

$$\phi_B \leq b$$

Therefore, in order to remain in region one, ϕ_B for the continuous pump must not exceed the b value. Or, using subscript c to designate continuous operation,

$$(\phi_{B\ max})_c = b \tag{3}$$

The second condition for achieving separation in region one is $L_2 \leqslant h$, or

$$\frac{Q(1 + \phi_B)}{A\epsilon(1 + m_o)(1 + b)} \frac{\pi}{\omega} \leqslant h$$

Note, π/ω is the minimum half cycle time necessary to achieve equilibrium. The limiting value of Q , corresponding to $L_2 = h$, for a given value of ϕ_B is thus,

$$(Q_{max})_c = \frac{hA\epsilon(1 + m_o)(1 + b)}{\frac{\pi}{\omega}(1 + \phi_B)} \tag{4}$$

Let $K_h = hA\epsilon(1 + m_o)(1 + b)/(\pi/\omega)$, which represents a constant experimental parameter of the system. Then

$$(Q_{max})_c = \frac{K_h}{1 + \phi_B} \tag{4a}$$

And for any value of Q_c less than $(Q_{max})_c$ (i. e., $L_2 < h$),

$$Q_c = \frac{K_i}{1 + \emptyset_B} \tag{4b}$$

where the subscript i (= 1,2,...) refers to a case where L_2 is less than h. Figure 7 is a plot of eqs. (4a) (curve A) and (4b) (curve B) on the Q-$\emptyset_B$ plane. The figure is bounded by the limiting conditions $0 \leqslant \emptyset_B \leqslant 1$ and $0 \leqslant Q \leqslant K_h$. Since curve A is the locus of maximum values of Q which the system can have in order to operate in region one, and b is the maximum value of $\emptyset_B$ for such operation, region one is shown as the shaded region with regions two and three corresponding to the regions shown in figure (B-5) (see appendix, pg. 73). The maximum flow rate of bottom product in region one for some $\emptyset_B$ is

$$P_{B\ \max(\emptyset_B)} = \emptyset_B Q_{\max} \tag{5}$$

or, combining eqs. (4a) and (5),

$$P_{B\ \max(\emptyset_B)} = \frac{K_h \emptyset_B}{1 + \emptyset_B} \tag{5a}$$

If the maximum value which $\emptyset_B$ can have for continuous pumping is substituted into eqs. (4a) and (5),

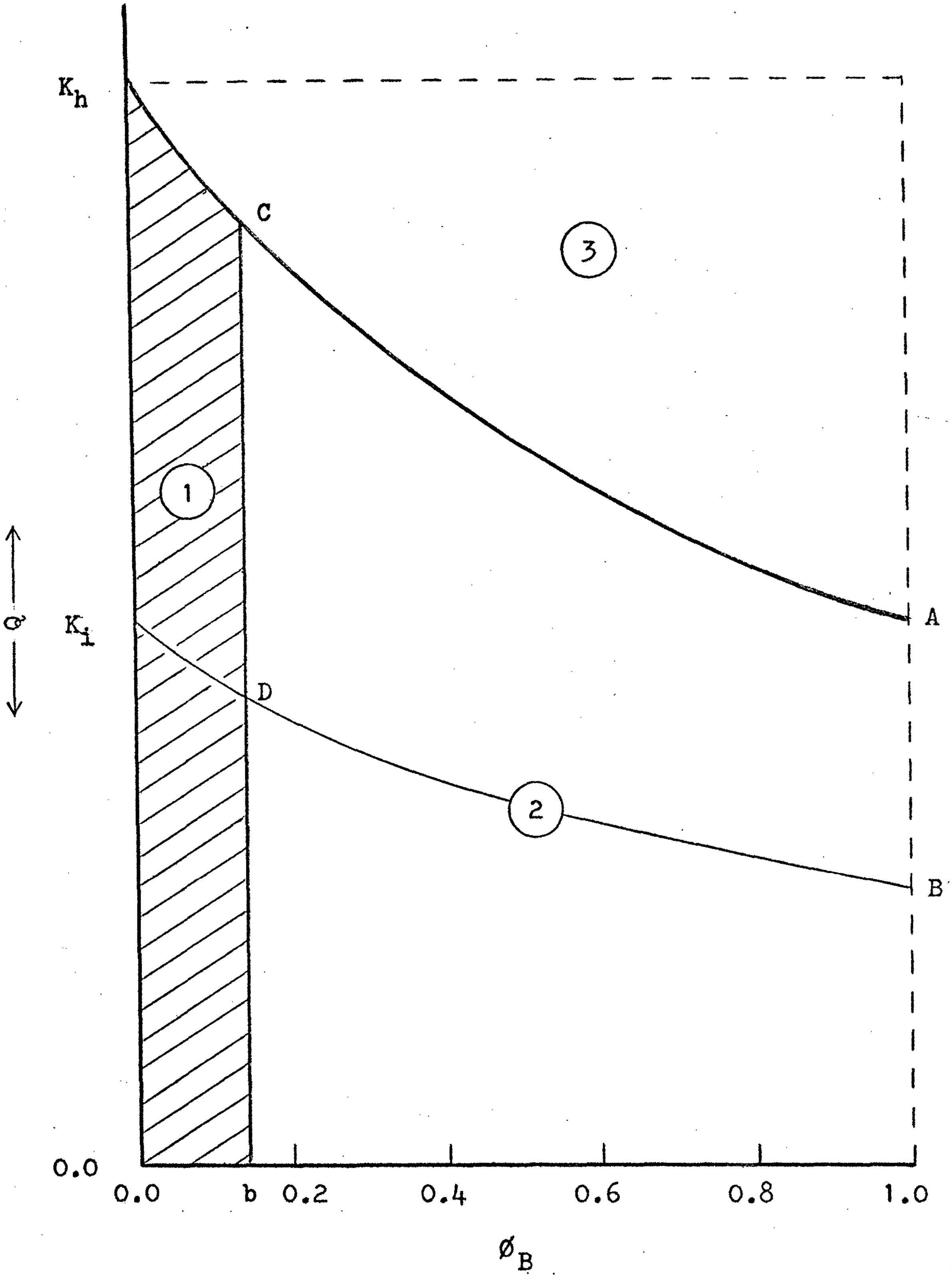

Figure 7 — The Three Regions of Operation Viewed on the Q-$\emptyset_B$ Plane for the Continuous Mode

$$(Q_{max})_c = \frac{K_h}{1 + b} \tag{5b}$$

and

$$(P_{B\ max(b)})_c = b(Q_{max})_c = \frac{K_h b}{1 + b} \tag{5c}$$

Since $0 \leqslant \phi_B \leqslant b$ in region one, let ϕ_B equal b/r, where r is any number greater one, so that $0 < \phi_B < b$. Then, from eq. (5a),

$$(P_{B\ max(\phi_B)})_c = \frac{K_h \frac{b}{r}}{1 + \frac{b}{r}} = \frac{K_h b}{r + b} \tag{5d}$$

Since $K_h b/(1 + b)$ is always greater than $K_h b/(r + b)$ it follows that the maximum bottom product flow rate for achieving complete removal of solute in the continuous pump will result if ϕ_B is equal to b and Q is equal to $K_h/(1 + b)$. This condition corresponds to point C in figure 7. If Q is less than Q_{max}, however, P_B will not be optimal (point D).

For the case of the semicontinuous pump (see appendix, pg. 70),

$$L_1 = \frac{Q}{A\epsilon(1 + m_o)(1 - b)} \frac{\pi}{\omega} \tag{6}$$

and
$$L_2 = \frac{Q(1 + \phi_B)}{A\epsilon(1 + m_o)(1 + b)} \frac{\pi}{\omega} \qquad (6a)$$

For operation in region one ($L_2 \leqslant L_1$),

$$\frac{1 + \phi_B}{1 + b} \leqslant \frac{1}{1 - b}$$

or
$$\phi_B \leqslant \frac{2b}{1 - b}$$

Using subscript s to designate semicontinuous operation,

$$(\phi_{B\ max})_s = \frac{2b}{1 - b} \qquad (7)$$

Since the quantity L_2 is given by the same expression for the continuous and semicontinuous cases, the second condition for achieving separation in region one ($L_2 \leqslant h$) as applied to semicontinuous pumping will lead to the same results for Q_{max} and $P_{B\ max}$ as before; namely,

$$(Q_{max})_s = \frac{K_h}{1 + \phi_B} \qquad (8)$$

and
$$(P_{B\ max})_s = \frac{K_h \phi_B}{1 + \phi_B} \qquad (9)$$

Substitution of eq. (7) into eqs. (8) and (9) gives,

$$(Q_{max})_s = \frac{K_h}{1 + \frac{2b}{1 - b}} = \frac{K_h(1 - b)}{1 + b} \tag{8a}$$

and

$$(P_{B\ max})_s = \frac{K_h \frac{2b}{1 - b}}{1 + \frac{2b}{1 - b}} = \frac{K_h 2b}{1 + b} \tag{9a}$$

Thus, in a similar manner as described for the continuous pump, the maximum bottom product rate for having complete removal of solute in the semicontinuous pump will result if ϕ_B is equal to $2b/(1 - b)$ and Q is equal to $K_h 2b/(1 + b)$. This condition corresponds to point E in figure 8.

Dividing eq. (5b) by eq. (8a) ,

$$\frac{(Q_{max})_c}{(Q_{max})_s} = \frac{1}{1 - b}$$

or

$$(Q_{max})_s = (1 - b)(Q_{max})_c \tag{10}$$

or in terms of displacement volume over a half cycle,

$$(Q_{max}\pi/\omega)_s = (1 - b)(Q_{max}\pi/\omega)_c \tag{10a}$$

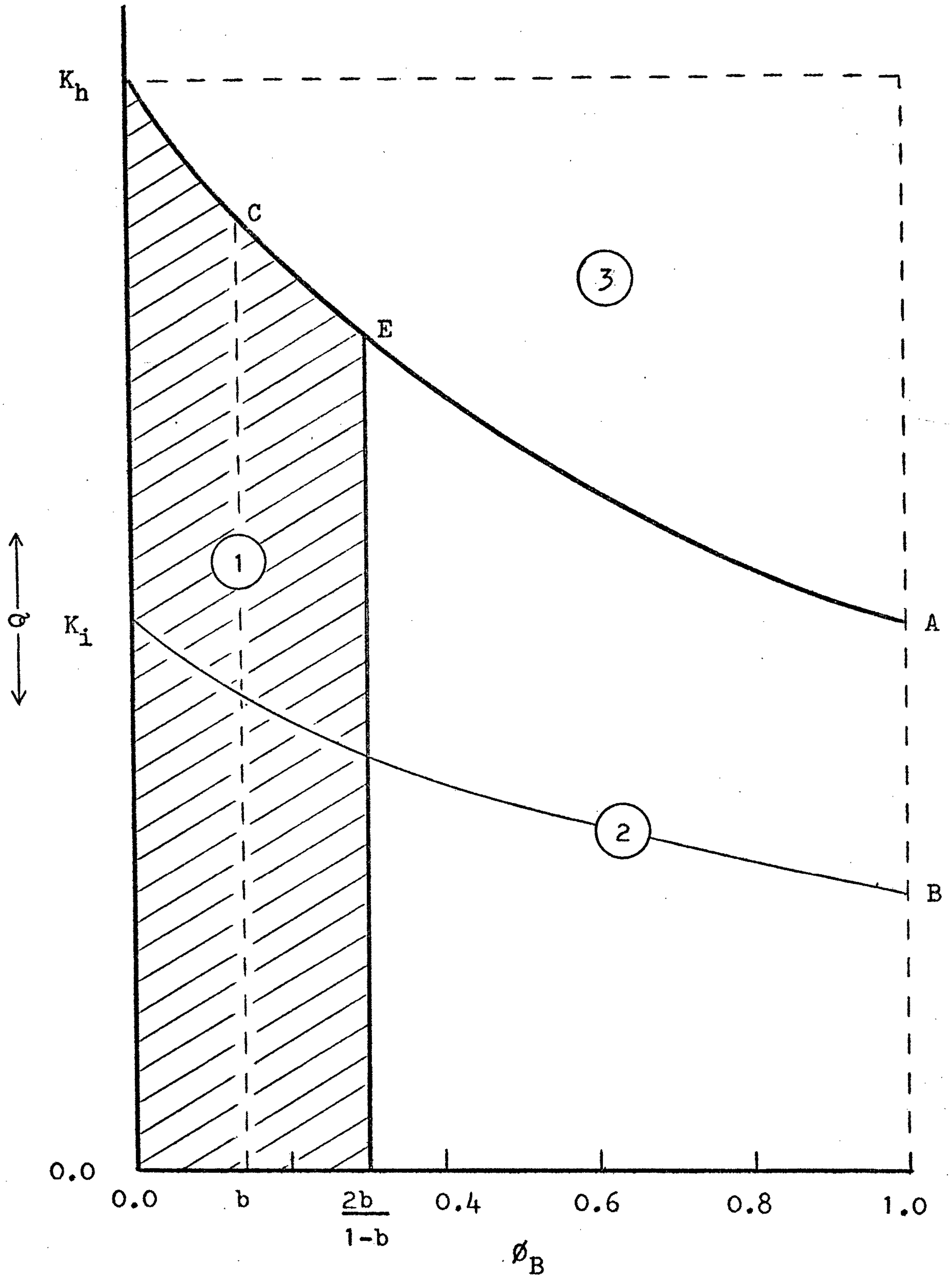

Figure 8 — The Three Regions of Operation Viewed on the Q-$\emptyset_B$ Plane for the Semicontinuous Mode

Dividing eq. (5c) by eq. (9a),

$$\frac{(P_{B\ max})_c}{(P_{B\ max})_s} = \frac{1}{2}$$

or

$$\frac{(P_{B\ max})_s}{2} = (P_{B\ max})_c \tag{11}$$

But since $(P_{B\ max})_s$ refers to the rate of bottom product removal during the cold half cycle only (the rate being zero during the hot half cycle), the value becomes $(P_{B\ max})_s/2$ as averaged over the entire cycle. Thus,

$$\langle P_{B\ max} \rangle_s = \langle P_{B\ max} \rangle_c \tag{11a}$$

with reference to a complete cycle. In terms of the average product volume collected during any half cycle,

$$\langle P_{B\ max}\, \pi/\omega \rangle_s = \langle P_{B\ max}\, \pi/\omega \rangle_c \tag{11b}$$

Hence, if the operating conditions for the two modes of parametric pumping are kept equal, the maximum possible amount of bottom product (with complete, eventual removal of solute) which can be collected over one full cycle is the same for the two kinds of pumps; but the maximum reservoir displacement rate corresponding to this optimal condition is smaller for the case of semicontinuous operation by a factor of (1 - b).

Now let $Q_c = Q_s$ be less than $(Q_{max})_s$ or $(Q_{max})_c$; and noting that $2\pi/\omega$ is the full cycle time,

$$\langle P_{B\ max} \rangle_s (2\pi/\omega) = \langle \phi_{B\ max} \rangle_s Q_s (2\pi/\omega) = \frac{bQ_s}{1 - b}(2\pi/\omega) \quad (12)$$

$$\langle P_{B\ max} \rangle_c (2\pi/\omega) = \langle \phi_{B\ max} \rangle_c Q_c (2\pi/\omega) = bQ_c (2\pi/\omega) \quad (12a)$$

Dividing eq. (12a) by eq. (12),

$$\frac{\langle P_{B\ max} \rangle_c}{\langle P_{B\ max} \rangle_s} = 1 - b$$

or

$$\langle P_{B\ max} \rangle_c = (1 - b) \langle P_{B\ max} \rangle_s \quad (13)$$

Therefore, if both pumps are operated with displacement rates which are less than the respective maximum values but equal to each other, the maximum amount of bottom product collected per cycle is smaller for the continuous pump by a factor of (1 - b).

This theory may be extended for multicomponent solutions. Assume that a dilute solution includes s adsorbable components in an inert solvent. Assume further that the solution may be treated as s pair of pseudo binary systems. Each system includes one solute and the common inert solvent, each with the dimensionless equilibrium parameter b_i and corresponding values of L_{1i} and L_{2i}. Furthermore,

$$b_1 > b_2 \ldots\ldots \quad b_k \geqslant \emptyset_B > b_{k+1} \ldots\ldots > b_s \qquad (14)$$

for the continuous pump, and

$$\left(\frac{2b}{1-b}\right)_1 > \left(\frac{2b}{1-b}\right)_2 \ldots\ldots \left(\frac{2b}{1-b}\right)_k \geqslant \emptyset_B > \left(\frac{2b}{1-b}\right)_{k+1} \ldots\ldots > \left(\frac{2b}{1-b}\right)_s \qquad (15)$$

for the semicontinuous pump. Also,

$$L_{2i} = \frac{Q(1 + \emptyset_B)}{A\epsilon(1 + b_i)(1 + m_o)} \frac{\pi}{\omega} \leqslant h \qquad (16)$$

for both pumps, where i = 1,2,..... k.

At steady state ($n \longrightarrow \infty$) the components i = 1,2,....k for which operations occur in region one would appear only in the top product stream, and the remaining components (k+1,....s) would appear in both the top and bottom product streams. In the extreme case where $k = s$ the bottom product would consist only of pure solvent, and the top product must contain all of the solutes supplied by the feed stream.

The optimal pump performance would be interpreted as the achievement of separation with maximum production of bottom product and complete removal of solutes 1,2, ... k. Thus, one can see from eqs. (14) to (16) that this would occur when

A) $L_{2k} = h$ (i.e., the pump is operated just on the verge of breakthrough of solute k from the bottom of the column), and

B) $\phi_B = b_k$ for the continuous pump.

$$\phi_B = \frac{2b_k}{1 - b_k} \text{ for the semicontinuous pump.}$$

Under these circumstances it follows from eqs. (5b) and (8a) that the maximum reservoir displacement flow rate is,

$$Q_{max} = \begin{cases} \dfrac{K_{hk}}{1 + b_k} = Ah\epsilon(1 + m_{ok})/(\pi/\omega) \\ \qquad \text{for the continuous pump} \\ \\ \dfrac{K_{hk}(1 - b_k)}{1 + b_k} = Ah\epsilon(1 + m_{ok})(1 - b_k)/(\pi/\omega) \\ \qquad \text{for the semicontinuous pump} \end{cases} \tag{17}$$

and the maximum bottom product flow rate is,

$$P_{B\,max} = \begin{cases} Q_{max} b_k = Ah\epsilon(1 + m_{ok}) b_k / (\pi/\omega) \\ \qquad \text{for the continuous pump} \\ Q_{max} \dfrac{2b}{1 - b} = Ah\epsilon(1 + m_{ok}) 2b_k / (\pi/\omega) \\ \qquad \text{for the semicontinuous pump} \end{cases} \tag{18}$$

For either continuous or semicontinuous modes operating in region one, the value of b for a particular component may be experimentally determined if the slope obtained from a plot of $\langle y_{BP2} \rangle_n / y_o$ (as calculated from eq. 1c) against the cycle number n, and the ratio C_2 between the bottom reservoir dead volume V_B and displacement rate Q are known (see appendix, pg. 76, eq. (C-1d)),

$$b = \frac{1 - 10^{\alpha} + C_2(1 - 10^{\alpha})}{1 + 10^{\alpha} - C_2(1 - 10^{\alpha})} \tag{C-1d}$$

or solving for the slope α,

$$\alpha = \log \left(\frac{\dfrac{1 - b}{1 + b} + C_2}{1 + C_2} \right) \tag{C-1b}$$

Assume that the hot and cold temperatures are fixed so that b, being a function of temperature only, remains constant. Since $(1 - b)/(1 + b)$ and C_2 are both less than one, the argument of eq. (C-1b) becomes less than one, and decreases with decreasing C_2 so that the absolute value of its log increases. Thus, the larger negative slope will result in a steeper line, which means that a smaller number of cycles is required to reach steady state (complete removal of solute). It is therefore desirable to minimize C_2; and since $C_2 = V_B/Q$, it follows that for a given dead volume, a minimum value of C_2 will result from the maximum value of Q. Hence, operating the pump with $Q = Q_{max}$ not only gives the maximum quantity of bottom product but also allows the greatest amount of separation from cycle to cycle, achieving steady state in the least amount of time.

RESULTS AND DISCUSSION

Experimental runs for determining the values of the system parameters b and m_o for the case of $NaNO_3$ separation from water using the ion retardation resin were carried out. Table 2 presents a list of all the experimental parameters for all runs made. Figure 9 shows a plot of the ratios of top and bottom concentrations for products collected during the cold half cycle to the feed concentration ($\langle y_{TP2} \rangle_n / y_o$ and $\langle y_{BP2} \rangle_n / y_o$ respectively) against the cycle number n for runs # 1,2, and 3. For run # 1 ($Q(\pi/\omega)$ = 20.0 cc) the slope α of the line was found to be -.0294, and the value of b calculated from eq. (C-1d) corresponding to this run was 0.0415. To check this value run # 2 was made, which was identical to run # 1 except that $Q(\pi/\omega)$ = 30.0 cc. As seen from figure 9 the resulting experimental points produced nearly the same line as that of run # 1 so that the slope essentially remained the same; and since the value of C_2 was identical for both cases, the value of b remained the same. Note that the run having the smaller value of C_2 resulted in a line having a steeper slope and consequently better separation from cycle to cycle. From the theory of parametric pumping developed by Chen and associates (1), values of $\langle y_{TP2} \rangle_n / y_o$ and $\langle y_{BP2} \rangle_n / y_o$ may be calculated from equations involving certain parameters, one of which being L_2. As eqs. (2a) and (6a) indicate, L_2 is directly proportional to $1/(1 + m_o)$. If different values of L_2 are assumed for a particular set of experimental parameters, and incerted into these equations, various curves for the top product concentration profile result; and the curve which best fits the experimental points corresponding to the same set of parameters will give the best value of L_2, from which m_o is then calculated. The best fit for the case of run # 1 corresponded to a value of L_2 equal to 50.0 cm., and m_o, calculated from eq. (2a) was 0.592.

From eq. (8a) $Q_{max}(\pi/\omega)$ for semicontinuous operation was calculated using the parameters of run # 1 and was found to be 34.56 cc., and $P_{B\ max}(\pi/\omega)$ as calculated from eq. (9a) was 2.88 cc. Figures 10 and 11 show experimental varification of these predicted maximum values. Figure 10 shows the effects of Q and P_B on the product concentrations for the semicontinuous pump. As long as $Q \leqslant Q_{max}$ (or $Q(\pi/\omega) \leqslant Q_{max}(\pi/\omega)$) and $P_B \leqslant P_{B\ max}$ (or $P_B(\pi/\omega) \leqslant P_{B\ max}(\pi/\omega)$), $\langle y_{BP2} \rangle / y_o$ decreases as n increases, and will approach zero as theory predicts (curves 1 and 3). If, in a pump originally operated in a region where $Q < Q_{max}$ and $P_B < P_{B\ max}$, P_B is increased until it exceeds $P_{B\ max}$ or Q becomes greater than Q_{max}, the steady state behavior of the pump abruptly switches from a mode in which solute is completely removed from the lower reservoir to one in which solute removal is incomplete (curves 4 and 5). Hence, Q_{max} and $P_{B\ max}$ are the operating conditions necessary to accomplish separation with the maximum production and infinite separation factors (defined as the top product concentration at steady state divided by the bottom product concentration at steady state). It should be pointed out that the crossing of the boundary $Q = Q_{max}$ or $P_B = P_{B\ max}$ may also be thought of as switching from regions one to three or one to two.

As shown in figure 11 the performance characteristics of both continuous and semicontinuous pumps are similar in nature. If the pumps are operated with $Q \leq Q_{max}$ and $P_B \leq P_{B\ max}$ (curves 2,3, and 6), the bottom product concentration decreases as n increases, and the separation factor becomes large as n becomes large. The principal difference between the two pumps is the difference in Q_{max} (eq. (10)). For the continuous pump Q_{max} is greater than that for the semicontinuous pump by a factor of $1/(1 - b_k)$. Therefore, for a large value of b_k, Q_{max} in the semicontinuous pump may become quite small relative to that in the continuous pump, i. e., one can have a much smaller reservoir volume by using semicontinuous operation. In terms of the average value of $P_{B\ max}$ over a complete cycle, however, both semicontinuous and continuous pumps have the same maximum bottom product flow rate. In all cases the experimental results were in close agreement to the calculated values for all regions involved.

Figure 12 shows the effect of temperature on the value of b. Run # 1, operated with hot and cold temperatures of

65.0°C and 5.0°C, resulted in a value of b equal to 0.0415 Run # 4, operated with a larger temperature difference (70.0°C and 2.0°C) produced a b value equal to 0.0474 . Since for greater temperature differences the value of b is larger, it follows from the equations for Q_{max} and $P_{B\ max}$ for both modes of pumping that these values are larger. Thus, for the case of larger b (with constant C_2), not only will the separation from cycle to cycle be better, but more bottom product for a given column height may be collected.

CONCLUSIONS

In this paper it has been shown both experimentally and theoretically that for a given column height, a maximum amount of solute free product corresponding to a maximum reservoir displacement rate may be collected from continuous and semicontinuous parametric pumps. When the product and displacement rates are both less than these maximum values, complete separation of solute from solution will eventually result. If one of these parameters is greater than the maximum value, however, only partial separation will occur. Although the average maximum product rate over a complete cycle was found to be the same for the two types of pumps, the maximum displacement rate of the semicontinuous pump was greater than that of the continuous pump by a factor of $1 - b_k$.

Although it is desirable to have the shortest possible cycle times, there exists a minimum cycle time in which equilibrium will be established in order that the theories developed here might hold. If a pump is operated at a cycle time which is shorter than the minimum the system may not reach equilibrium, and the simple equilibrium theory upon which all further development is based may not be assumed. Thus, the optimal parametric pump performance will result from the use of a semicontinuous pump operating with a maximum displacement rate, the minimum cycle time, and a maximum possible difference in hot and cold temperature.

As the experimental results have shown the $NaNO_3$ - H_2O system was an equilibrium system. Similar experiments using a NaCl - H_2O system have been carried out elsewhere, and it was found that regardless of the operating conditions, complete separation of salt from water was impossible. It was subsequently hypothesized that this system was not an equilibrium system. One may wonder what the nature of the difference between these two systems is. Experiments have shown that the b value of the NaCl - H_2O system is more than three times that of the $NaNO_3$ - H_2O system for the same temperature differences. This means that more chloride ions will adsorb onto the resin as a result of temperature change than will the nitrate ions. This seems reasonable since the nitrate ions are much bulkier than the chloride ions, and thus might have trouble attaching themselves to all available exchange sites. The system having more ion adsorbtion, however, will require a longer minimum cycle time for the achievement of equilibrium than will a system whose ions do not adsorb as well. Consequently, for the same cycle time, better separation from cycle to cycle in the case of the NaCl system would be observed in the first few cycles, but only partial separation could be accomplished at steady state regardless of the parameters used. The $NaNO_3$ system, however, as this paper has shown, was capable of complete solute removal under certain conditions. It therefore seems that systems having relatively smaller values of b will have much better steady state separations for a given cycle time.

NOMENCLATURE

a = the difference between m_h or m_c and m_o

b = a measure of the extent of adsorbtive capacity of solute as a result of temperature change, dimensionless

C_1 = the ratio of the top reservoir dead volume to the displacement, dimensionless

C_2 = the ratio of the bottom reservoir dead volume to the displacement, dimensionless

D = mass diffusivity of solute

h = column height, cm.

K = a value equal to an important parameter group of the system

L = penetration distance of a concentration front, cm.

M = thermal equilibrium constant equal to x/y

m = equilibrium parameter directly proportional to M

n = cycle number

P = product rate, cc./min.

Q = reservoir displacement, cc./min.

R = resistivity, ohms

T = temperature, °C

t = time, min.

v = interstitial velocity, cm./min.

V = reservoir dead volume, cc.

x = concentration of solute in the solid phase, g-moles/gr.

y = concentration of solute in the liquid phase, g-moles/cc.

z = distance along the length of the column, cm.

$\langle\,\rangle$ = average value

Greek Letters:

α = slope of line on plot of $\log(\langle y_{BP2} \rangle_n / y_o)$ vs. n

ρ_s = density of solute, g/cc.

ρ_f = density of fluid, g/cc.

ϵ = void fraction in packing, dimensionless

ϕ = product volumetric flow rate divided by the reservoir displacement rate, dimensionless

$\frac{\pi}{\omega}$ = duration of half cycle, min.

Subscripts:

o = property at the average temperature of a complete cycle

1 = upflow or hot half cycle

2 = downflow or cold half cycle

c = continuous operation

s = semicontinuous operation

B = stream from or to the bottom of the column

T = stream from or to the top of the column

BP = bottom product

TP = top product

REFERENCES

(1) H. T. Chen and F. B. Hill. *Separation Science*, *6* (3), 411 (1971).

(2) H. T. Chen, J. L. Rak, J. D. Stokes, and F. B. Hill. *AIChE J.* *18*, 356 (1972).

(3) Grava, Sigurd. *Urban Planning Aspects of Water Pollution Controll*, 47 (1969).

(4) R. L. Pigford, B. Baker, and D. E. Blum. *Ind. Eng. Chem. Fundam.*, *8*, 144 (1969).

APPENDIX I

Tables and Graphs of Experimental Data

TABLE 1

Calibration Data

$NaNO_3$ concentration (moles/liter)	Resistance Reading (Ohms)
0.10	86.5
0.09	94.5
0.08	105.5
0.07	121.5
0.06	138.2
0.05	162.9
0.04	201.6
0.03	264.8
0.02	391.0
0.016	489.0
0.012	640.0
0.010	760.0
0.0080	950.0
0.0060	1250.0
0.0040	1850.0
0.0030	2383.0
0.0020	3600.0
0.0010	7000.0
0.00080	8470.0
0.00060	11100.0
0.00040	16510.0
0.00020	27070.0

TABLE 2

A List of Important Experimental Parameters for all Runs

Run	Mode	$Q(\frac{\pi}{\omega})$ (cc)	T_1 ($^\circ$C)	T_2 ($^\circ$C)	V_B (cc)	V_T (cc)	$\frac{\pi}{\omega}$ (min)	$Q(\phi_B+\phi_T)\frac{\pi}{\omega}$ (cc)	$P_B\frac{\pi}{\omega}$ (cc)	h (cm)	y_o (M)
1	s	20.0	65.0	5.0	5.00	5.00	20.0	5.00	1.00	90.	.0202
2	s	30.0	65.0	5.0	6.45	5.00	20.0	5.00	1.00	90.	.0263
3	s	30.0	65.0	5.0	4.30	5.00	20.0	5.00	1.00	90.	.0262
4	s	20.0	70.0	2.0	5.00	5.00	20.0	5.00	1.00	90.	.0285
5	s	30.0	65.0	5.0	4.30	5.00	20.0	5.00	2.00	90.	.0215
6	s	30.0	65.0	5.0	4.30	5.00	20.0	5.00	4.00	90.	.0258
7	s	40.0	65.0	5.0	5.00	5.00	20.0	5.00	1.80	90.	.0233
8	c	30.0	65.0	5.0	4.30	5.00	20.0	5.00	1.00	90.	.0242
9	c	30.0	65.0	5.0	4.30	5.00	20.0	5.00	2.00	90.	.0254

TABLE 3

Experimental Results of Run # 1

L_1 = 51.59 cm. L_2 = 50.00 cm.   Region One

n	R_{BP} (diluted)	R_{TP} (diluted)	$\langle y_{BP}\rangle_n$ X10^4 (diluted)	$\langle y_{TP}\rangle_n$ X10^4 (diluted)	$\langle y_{BP}\rangle_n / y_o$	$\langle y_{TP}\rangle_n / y_o$
1	—	—	—	—	—	—
2	37100.	16130.	1.73	4.12	.865	1.04
3	38750.	15610.	1.65	4.28	.825	1.08
4	44200.	15003.	1.44	4.44	.720	1.12
5	45000.	14802	1.42	4.52	.710	1.14
6	47000.	14740.	1.35	4.56	.675	1.15
7	50800.	14501	1.25	4.59	.625	1.16
8	53900.	14497	1.18	4.59	.590	1.16
9	57700.	14433	1.09	4.63	.545	1.17
10	63000.	14429	1.00	4.63	.500	1.17
11	64000.	14427	.981	4.67	.490	1.18
12	69500.	14424	.902	4.71	.450	1.19
13	77700.	14412	.801	4.75	.400	1.20
14	81500.	14399	.759	4.79	.380	1.21
15	90500.	13821	.751	4.87	.375	1.23
16	91200.	14403	.678	4.79	.340	1.21

TABLE 4

Experimental Results of Run # 2

L_1 = 78.13 cm. L_2 = 50.00 cm. Region One

n	R_{BP} (diluted)	R_{TP} (diluted)	$\langle y_{BP_n}\rangle$ $X10^4$ (diluted)	$\langle y_{TP_n}\rangle$ $X10^4$ (diluted)	$\langle y_{BP_n}\rangle / y_o$	$\langle y_{TP_n}\rangle / y_o$
1	28000.	12200.	2.32	5.52	.980	1.07
2	27700.	11500.	2.30	5.83	.885	1.13
3	31800.	11200.	2.04	5.98	.784	1.16
4	33800.	11050.	1.92	6.09	.739	1.18
5	36000.	10700.	1.78	6.24	.682	1.21
6	36400.	10600.	1.76	6.34	.674	1.23
7	40000.	10400.	1.60	6.45	.615	1.25
8	43400.	10250.	1.47	6.55	.564	1.27
9	44200.	10200.	1.44	6.60	.552	1.28
10	48200.	10150.	1.32	6.65	.506	1.29
11	52800.	9990.	1.20	6.76	.462	1.31
12	53300.	10050.	1.18	6.76	.455	1.31
13	57500.	10020.	1.08	6.76	.414	1.31
14	59100.	9950.	1.07	6.81	.410	1.32
15	64500.	9950.	.969	6.81	.372	1.32
16	71600.	9900.	.870	6.86	.334	1.33

TABLE 5

Experimental Results of Run # 3

L_1 = 78.13 cm. L_2 = 74.04 cm. Region One

n	R_{BP} (diluted)	R_{TP} (diluted)	$\langle y_{BPn}\rangle$ X10^4 (diluted)	$\langle y_{TPn}\rangle$ X10^4 (diluted)	$\langle y_{BPn}\rangle / y_o$	$\langle y_{TPn}\rangle / y_o$
1	28000.	12700.	2.32	5.29	.895	1.03
2	30800.	11400.	2.10	5.91	.810	1.15
3	33000.	11100.	1.96	6.06	.755	1.18
4	35500.	11000.	1.80	6.16	.694	1.20
5	38800.	10550.	1.65	6.42	.637	1.25
6	41200.	10300.	1.54	6.52	.593	1.27
7	42200.	10100.	1.51	6.68	.582	1.30
8	47000.	10280.	1.35	6.52	.522	1.27
9	48900.	10500.	1.30	6.73	.501	1.31
10	52900.	9970.	1.21	6.78	.468	1.32
11	57000.	9800.	1.12	6.93	.433	1.35
12	60000.	9950.	1.05	6.78	.403	1.32
13	62900.	10700.	.996	6.68	.384	1.30
14	68100.	10700.	.921	6.73	.355	1.31
15	74200.	10400.	.838	6.73	.323	1.31
16	75800.	9960.	.822	6.78	.317	1.32

TABLE 6

Experimental Results of Run # 4

L_1 = 52.36 cm. L_2 = 50.00 cm. Region One

n	R_{BP} (diluted)	R_{TP} (diluted)	$\langle y_{BP_n}\rangle$ X10^4 (diluted)	$\langle y_{TP_n}\rangle$ X10^4 (diluted)	$\langle y_{BP_n}\rangle/y_o$	$\langle y_{TP_n}\rangle/y_o$
1	25800.	11500.	2.54	5.87	.901	1.05
2	28000.	11200.	2.35	6.04	.832	1.08
3	30200.	11000.	2.14	6.15	.759	1.10
4	32100.	10750.	2.00	6.26	.708	1.12
5	34000.	10700.	1.90	6.31	.673	1.13
6	35700.	10300.	1.80	6.54	.638	1.17
7	40070.	10250.	1.59	6.59	.564	1.18
8	44000.	10200.	1.45	6.65	.513	1.19
9	49100.	10010.	1.28	6.76	.453	1.21
10	51400.	9910.	1.23	6.82	.436	1.22
11	54000.	9905	1.17	6.82	.415	1.22
12	58200.	9895	1.08	6.88	.381	1.23
13	60300.	9640.	1.04	6.98	.368	1.25
14	66000.	9600.	.942	7.04	.334	1.26
15	69400.	9510.	.900	7.10	.319	1.27
16	76500.	9450.	.807	7.15	.286	1.28

TABLE 7

Experimental results of Run # 5

L_1 = 78.13 cm. L_2 = 76.93 cm. Region One

n	R_{BP} (diluted)	R_{TP} (diluted)	$\langle y_{BP} \rangle_n$ X10 ^{4} (diluted)	$\langle y_{TP} \rangle_n$ X10^4 (diluted)	$\langle y_{BP} \rangle_n / y_o$	$\langle y_{TP} \rangle_n / y_o$
1	32800.	14900.	1.97	4.47	.925	1.06
2	35200.	14200.	1.82	4.68	.854	1.11
3	38300.	13800.	1.67	4.85	.783	1.15
4	40000.	13100.	1.60	5.14	.750	1.22
5	46200.	13050.	1.37	5.14	.676	1.22
6	46180.	12700.	1.37	5.27	.644	1.25
7	54300.	12600.	1.28	5.31	.603	1.26
8	51300.	12200.	1.23	5.52	.580	1.31
9	57200.	11800.	1.10	5.65	.517	1.34
10	61200.	11750.	1.03	5.73	.485	1.36
11	64400.	11700.	.996	5.69	.468	1.35
12	70050.	11600.	.894	5.78	.420	1.37
13	73500.	11400.	.854	5.94	.401	1.41
14	76700.	11200.	.813	6.03	.382	1.43
15	76750.	11150.	.811	6.03	.381	1.43
16	85000.	11000.	.732	6.15	.344	1.46

TABLE 8

Experimental Results of Run # 6

L_1 = 78.13 cm. L_2 = 81.73 cm. Region Two

n	R_{BP} (diluted)	R_{TP} (diluted)	$\langle y_{BP_n} \rangle$ X10^4 (diluted)	$\langle y_{TP_n} \rangle$ X10^4 (diluted)	$\langle y_{BP_n} \rangle / y_o$	$\langle y_{TP_n} \rangle / y_o$
1	27200.	12200.	2.39	5.56	.935	1.10
2	28300.	11200.	2.28	6.02	.894	1.19
3	29500.	10700.	2.18	6.32	.854	1.25
4	31200.	10400.	2.06	6.48	.808	1.28
5	32000.	10000.	2.02	6.78	.792	1.32
6	34400.	10020.	1.87	6.73	.734	1.33
7	34350.	9800.	1.87	6.88	.733	1.36
8	34200.	10030.	1.88	6.73	.735	1.33
9	35400.	9940	1.80	6.83	.706	1.35
10	37800.	9795	1.70	6.88	.667	1.36
11	37750.	9985	1.71	6.78	.671	1.34
12	38000.	9930.	1.68	6.83	.657	1.35
13	39000.	9620.	1.64	6.93	.643	1.37
14	38800.	9785	1.65	6.88	.645	1.36
15	40000.	9787	1.59	6.88	.623	1.36
16	41000.	9620.	1.56	6.93	.610	1.37

TABLE 9

Experimental Results of Run # 7

L_1 = 104.17 cm. L_2 = 100.48 cm.   Region Three

n	R_{BP} (diluted)	R_{TP} (diluted)	$\langle y_{BP_n} \rangle$ X10^4 (diluted)	$\langle y_{TP_n} \rangle$ X10^4 (diluted)	$\langle y_{BP_n} \rangle / y_o$	$\langle y_{TP_n} \rangle / y_o$
1	29900.	14010.	2.17	4.80	.940	1.05
2	31800.	13700.	2.03	4.89	.878	1.07
3	31850.	13400.	2.02	5.03	.875	1.10
4	33800.	13000.	1.91	5.16	.829	1.13
5	36000.	12800.	1.78	5.25	.771	1.15
6	36050.	12650.	1.78	5.30	.770	1.16
7	36800.	12780.	1.76	5.25	.761	1.15
8	38200.	12770.	1.67	5.25	.722	1.15
9	39100.	11700.	1.63	5.76	.708	1.16
10	38900.	12500.	1.64	5.35	.709	1.17
11	39800.	12900.	1.62	5.39	.701	1.18
12	39900.	11690.	1.61	5.76	.698	1.16
13	40100.	12480.	1.59	5.35	.690	1.17
14	40000.	12500.	1.60	5.35	.692	1.17
15	40010.	12510.	1.60	5.35	.695	1.17
16	39850.	11710.	1.61	5.76	.699	1.16

TABLE 10

Experimental Results of Run # 8

L_1 = 75.52 cm. L_2 = 74.52 cm. Region One

n	R_{BP} (diluted)	R_{TP} (diluted)	$\langle y_{BP} \rangle_n$ X10^4 (diluted)	$\langle y_{TP} \rangle_n$ X10^4 (diluted)	$\langle y_{TP} \rangle_n / y_o$	$\langle y_{TP} \rangle_n / y_o$
1	30000.	13600.	2.16	4.93	.900	1.04
2	32000.	13250.	2.02	5.08	.841	1.07
3	34200.	13100.	1.88	5.12	.784	1.08
4	35500.	12700.	1.81	5.31	.755	1.12
5	38300.	12300.	1.67	5.46	.695	1.15
6	42000.	12200.	1.52	5.50	.634	1.16
7	46000.	12000.	1.38	5.60	.576	1.18
8	45800.	12010.	1.36	5.60	.567	1.18
9	48800.	11200.	1.30	5.72	.544	1.21
10	52900.	11500.	1.20	5.84	.500	1.23
11	57600.	11300.	1.09	5.93	.455	1.25
12	64200.	11320.	.975	5.93	.407	1.25
13	68400.	11400.	.910	5.88	.380	1.24
14	70300.	11310.	.882	5.93	.368	1.25
15	76600.	11200.	.815	6.03	.340	1.27
16	80000.	11300.	.774	5.93	.323	1.25

TABLE 11

Experimental Results of Run # 9

L_1 = 72.92 cm. L_2 = 76.93 cm. Region Two

n	R_{BP} (diluted)	R_{TP} (diluted)	$\langle y_{BP} \rangle_n$ X10^4 (diluted)	$\langle y_{TP} \rangle_n$ X10^4 (diluted)	$\langle y_{BP} \rangle_n / y_o$	$\langle y_{TP} \rangle_n / y_o$
1	28000.	12800.	2.33	5.28	.928	1.06
2	29100.	12400.	2.24	5.43	.891	1.09
3	31000.	12100.	2.08	5.53	.828	1.11
4	32200.	12020.	1.98	5.58	.789	1.12
5	33400.	11800.	1.91	5.63	.759	1.13
6	35300.	11650.	1.81	5.68	.720	1.14
7	37200.	11500.	1.73	5.88	.688	1.18
8	37250.	11200.	1.72	6.00	.684	1.20
9	39000.	10900.	1.64	6.18	.653	1.24
10	42200.	10700.	1.50	6.28	.598	1.26
11	42200.	10600.	1.50	6.37	.597	1.28
12	42150.	10400.	1.51	6.52	.599	1.31
13	43100.	10550.	1.48	6.42	.590	1.29
14	43700.	10200.	1.47	6.62	.585	1.33
15	43700.	10150.	1.47	6.67	.583	1.34
16	43750.	10120.	1.46	6.72	.581	1.35

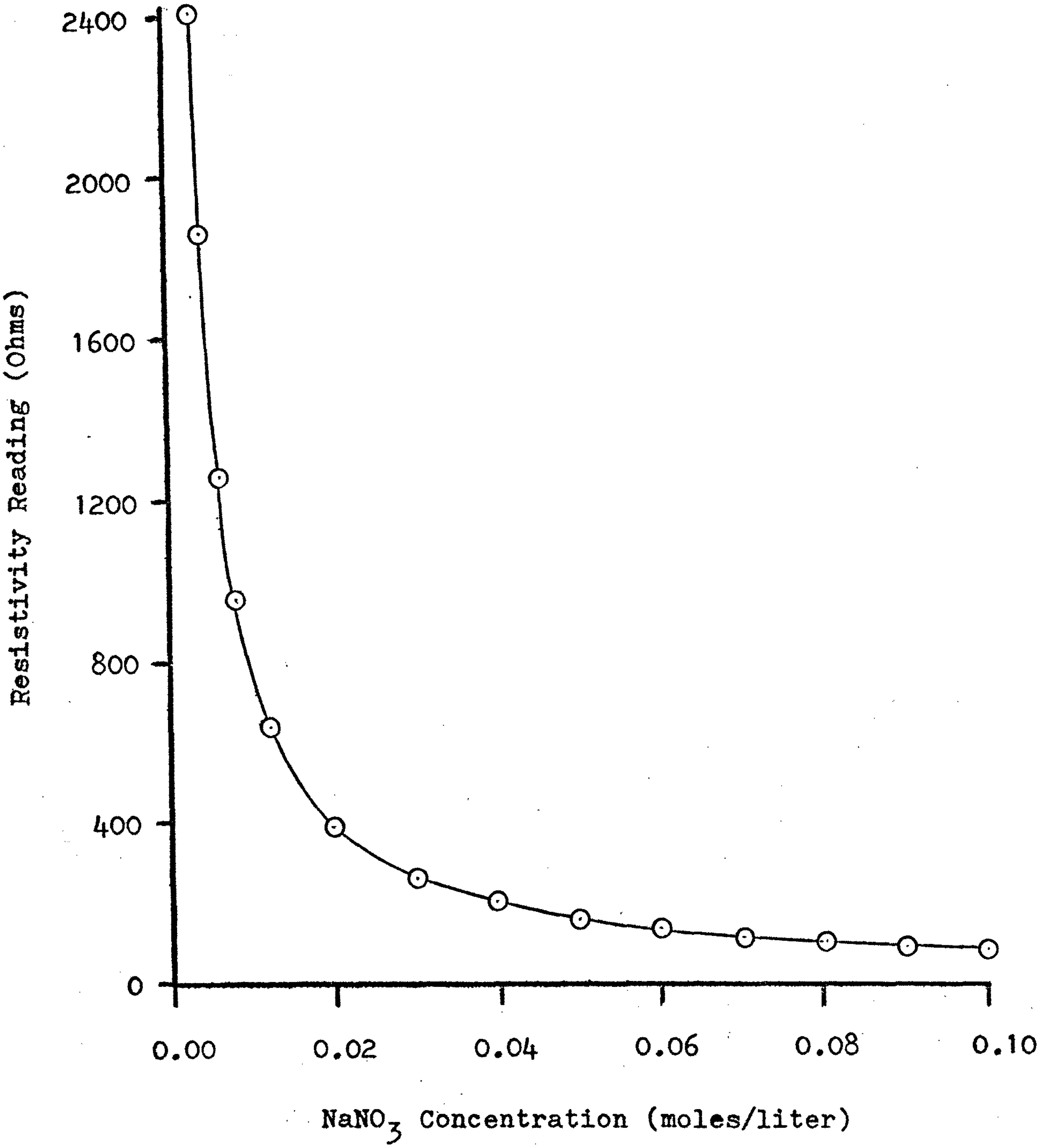

Figure 2 — Resistivity of NaNO$_3$ Solutions Against Concentration

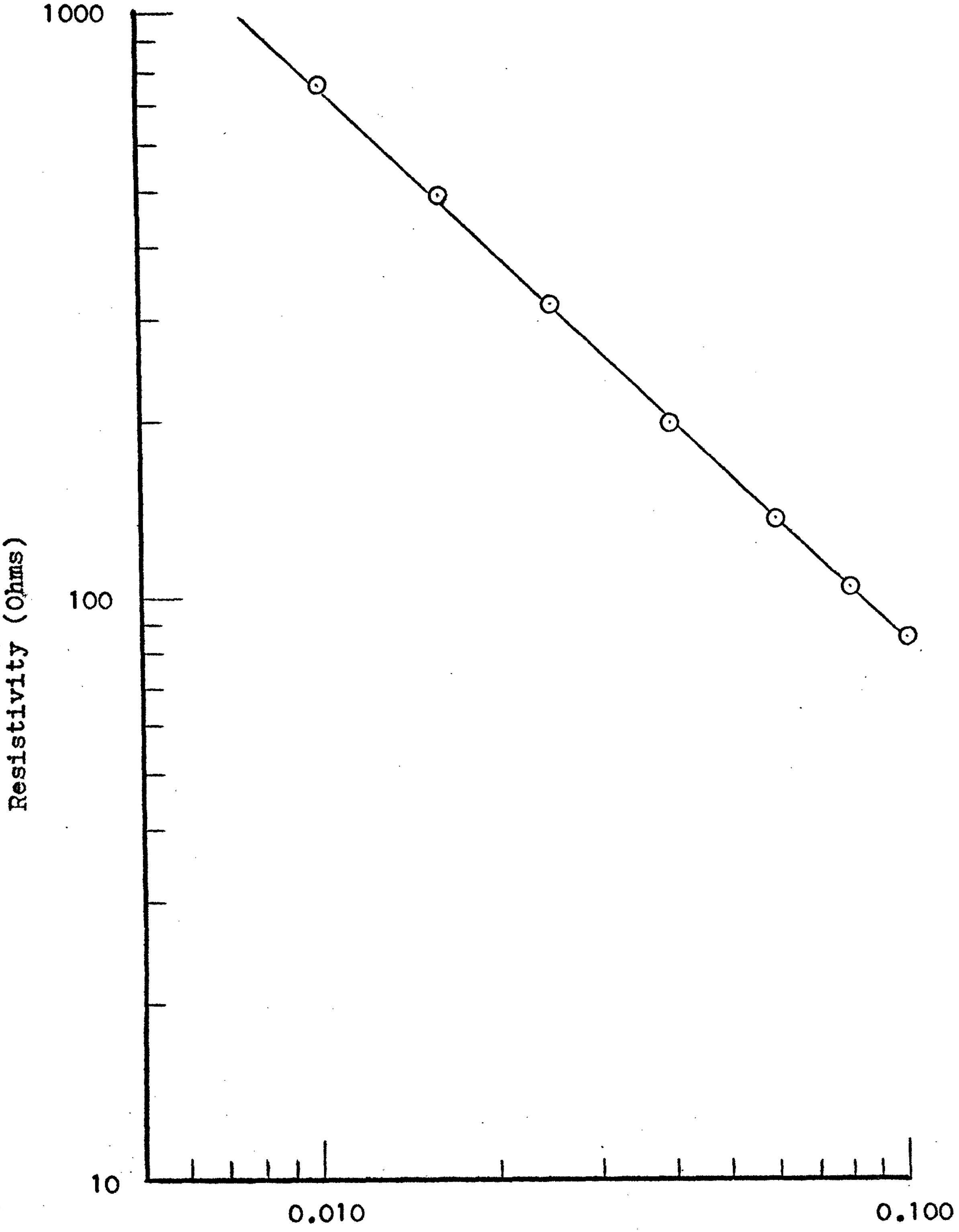

Figure 3 — Calibration Curve of Resistivity for 0.010 to 0.100 molar NaNO$_3$ Solutions

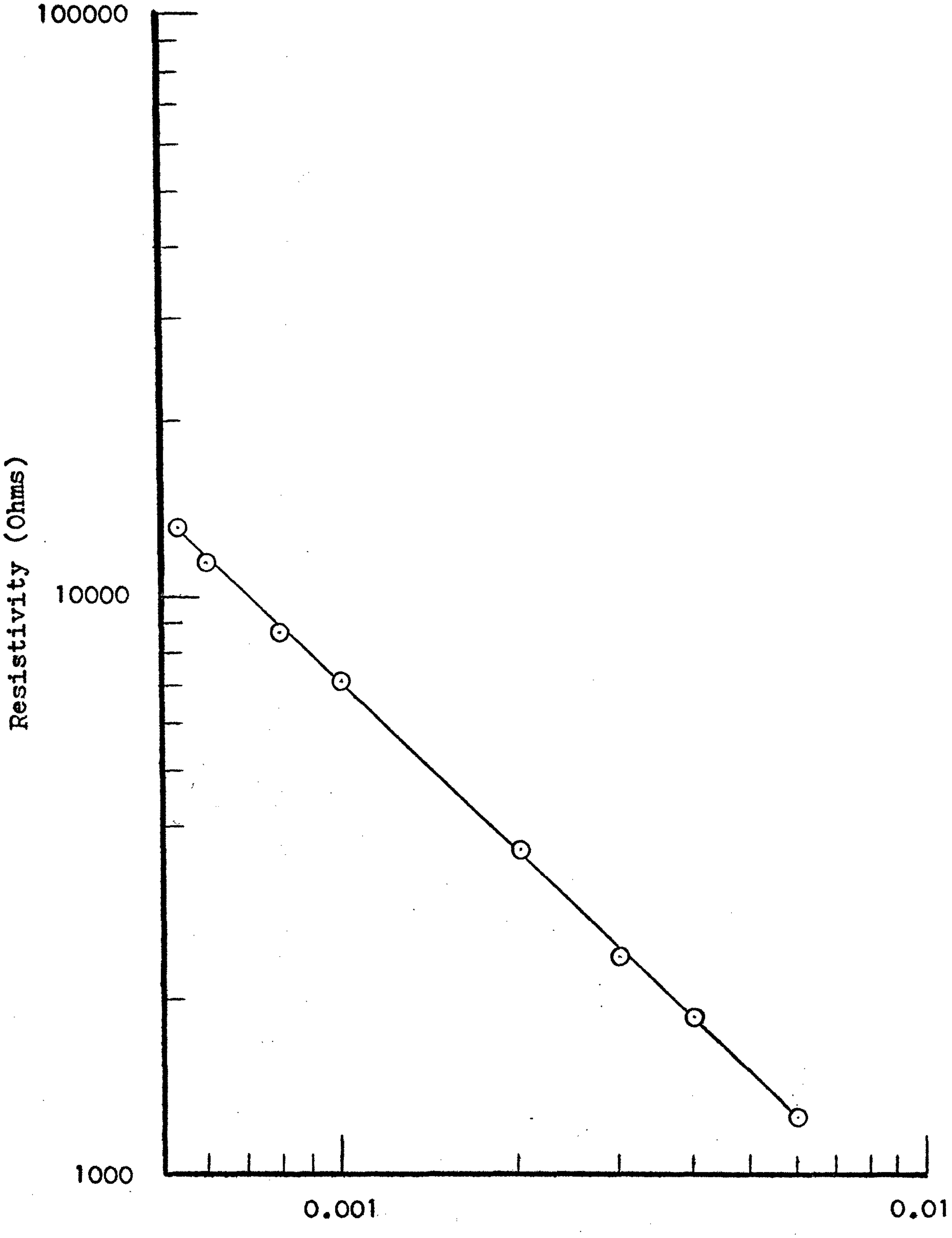

NaNO$_3$ Concentration (moles/liter)

Figure 4 — Calibration Curve of Resistivity for 0.001 to 0.01 molar NaNO$_3$ Solutions

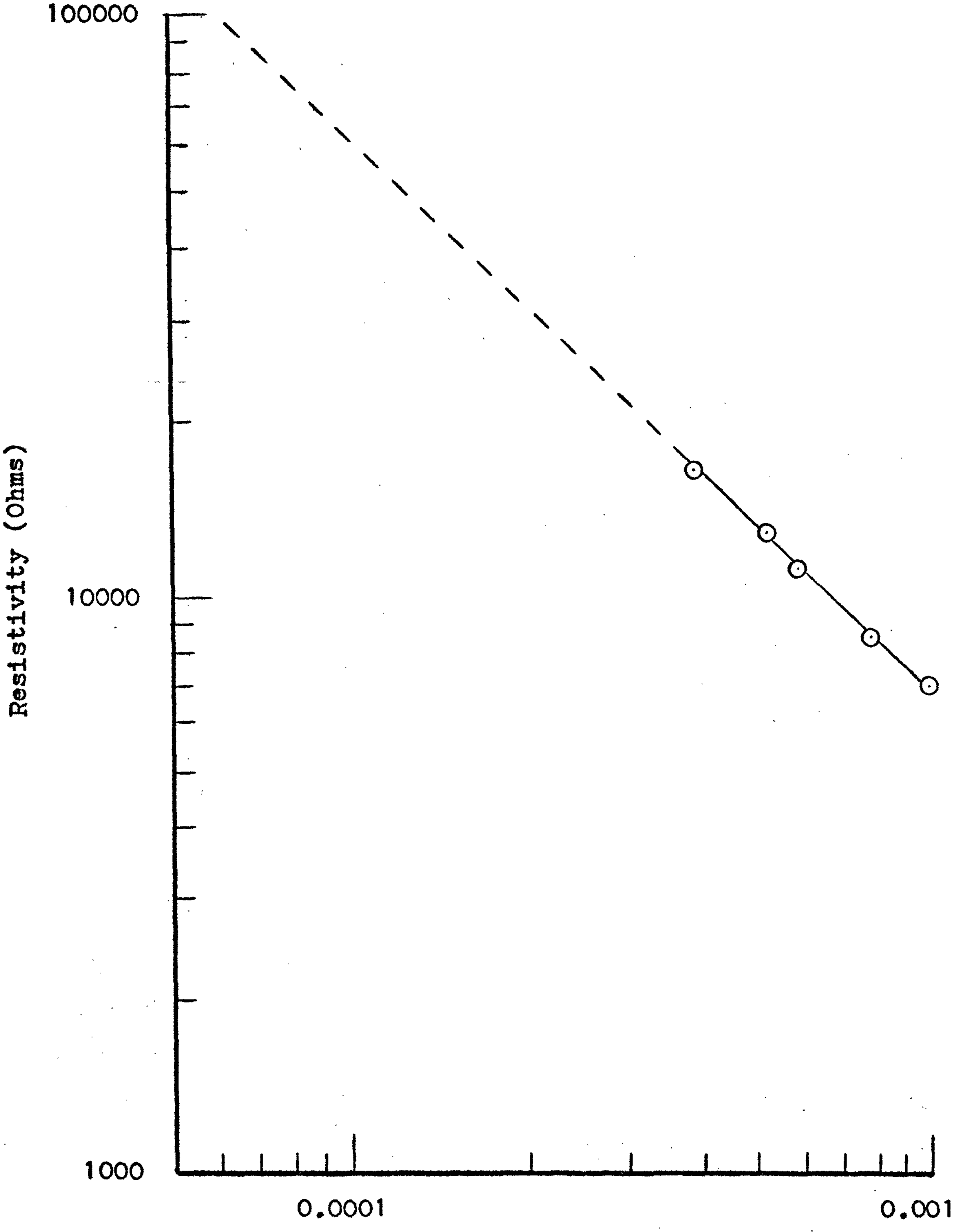

Figure 5 — Calibration Curve of Resistivity for 0.0001 to 0.001 molar NaNO$_3$ Solutions

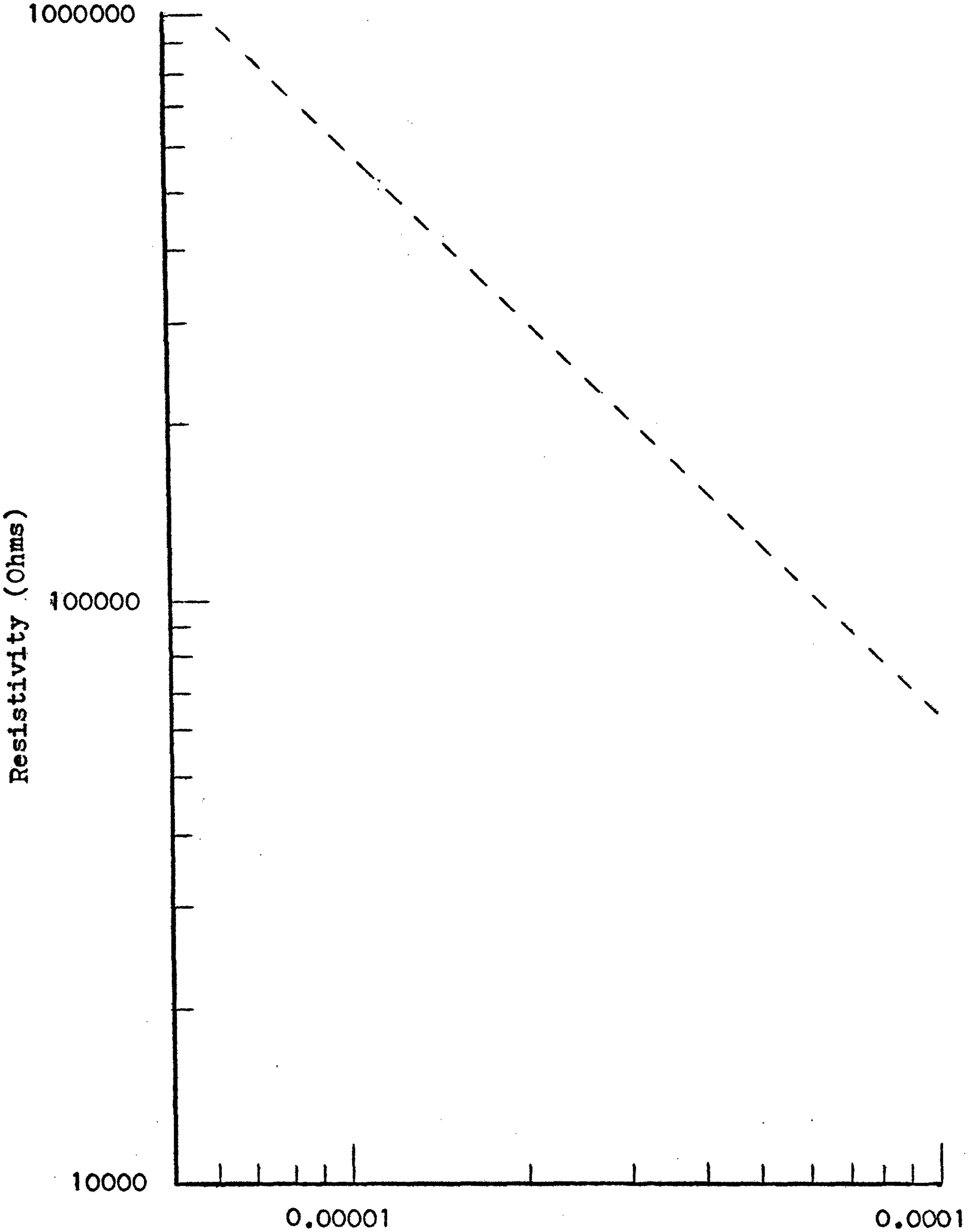

NaNO$_3$ Concentration (moles/liter)

Figure 6 — Calibration Curve of Resistivity for 0.00001 to 0.0001 molar NaNO$_3$ Solutions

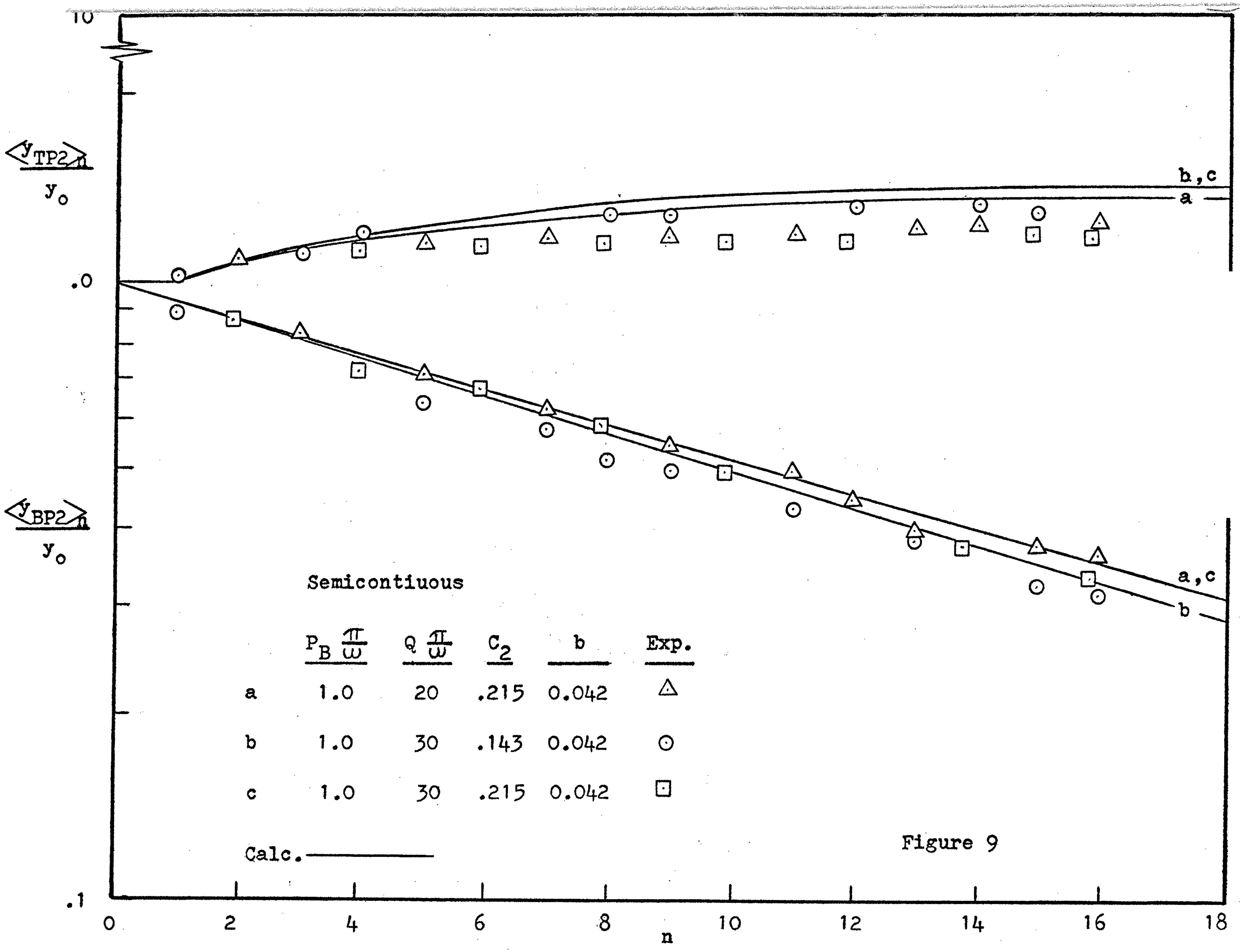
10
$\frac{\langle y_{TP2} \rangle_n}{y_o}$
.0
$\frac{\langle y_{BP2} \rangle_n}{y_o}$
.1
0
2
4
6
8
10
12
14
16
18
n
b,c
a
a,c
b
Semicontiuous
$P_B \frac{\pi}{\omega}$
$Q \frac{\pi}{\omega}$
C_2
b
Exp.
a 1.0 20 .215 0.042 △
b 1.0 30 .143 0.042 ⊙
c 1.0 30 .215 0.042 ⊡
Calc. ———

Figure 9

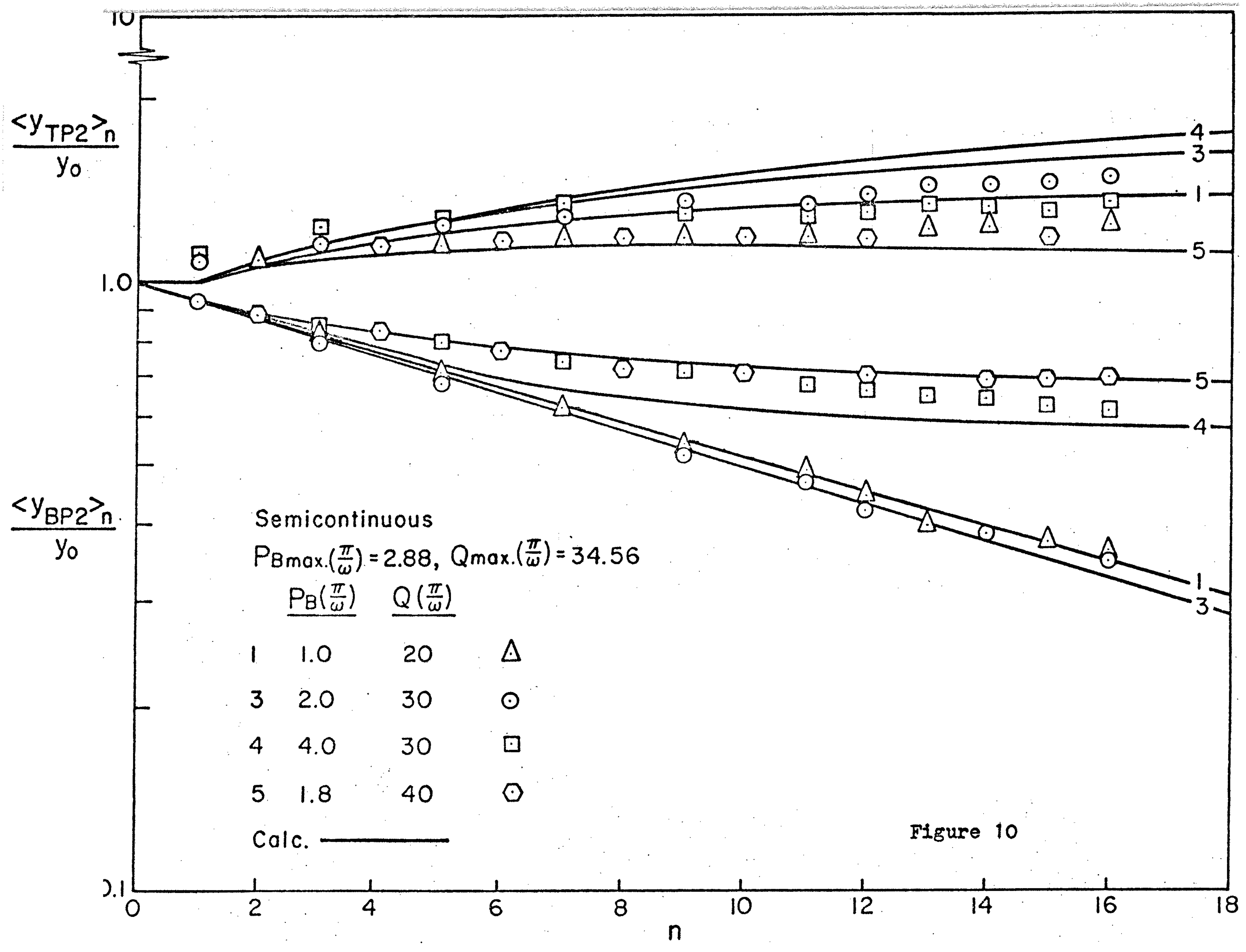
10
1.0
0.1
$\frac{\langle y_{TP2} \rangle_n}{y_0}$
$\frac{\langle y_{BP2} \rangle_n}{y_0}$
0
2
4
6
8
10
12
14
16
18
n
4
3
1
5
5
4
1
3
Semicontinuous
$P_{B\max}(\frac{\pi}{\omega}) = 2.88$, $Q_{\max}(\frac{\pi}{\omega}) = 34.56$
$P_B(\frac{\pi}{\omega})$ $Q(\frac{\pi}{\omega})$
1 1.0 20 △
3 2.0 30 ⊙
4 4.0 30 ⊡
5 1.8 40 ⬡
Calc. ——

Figure 10

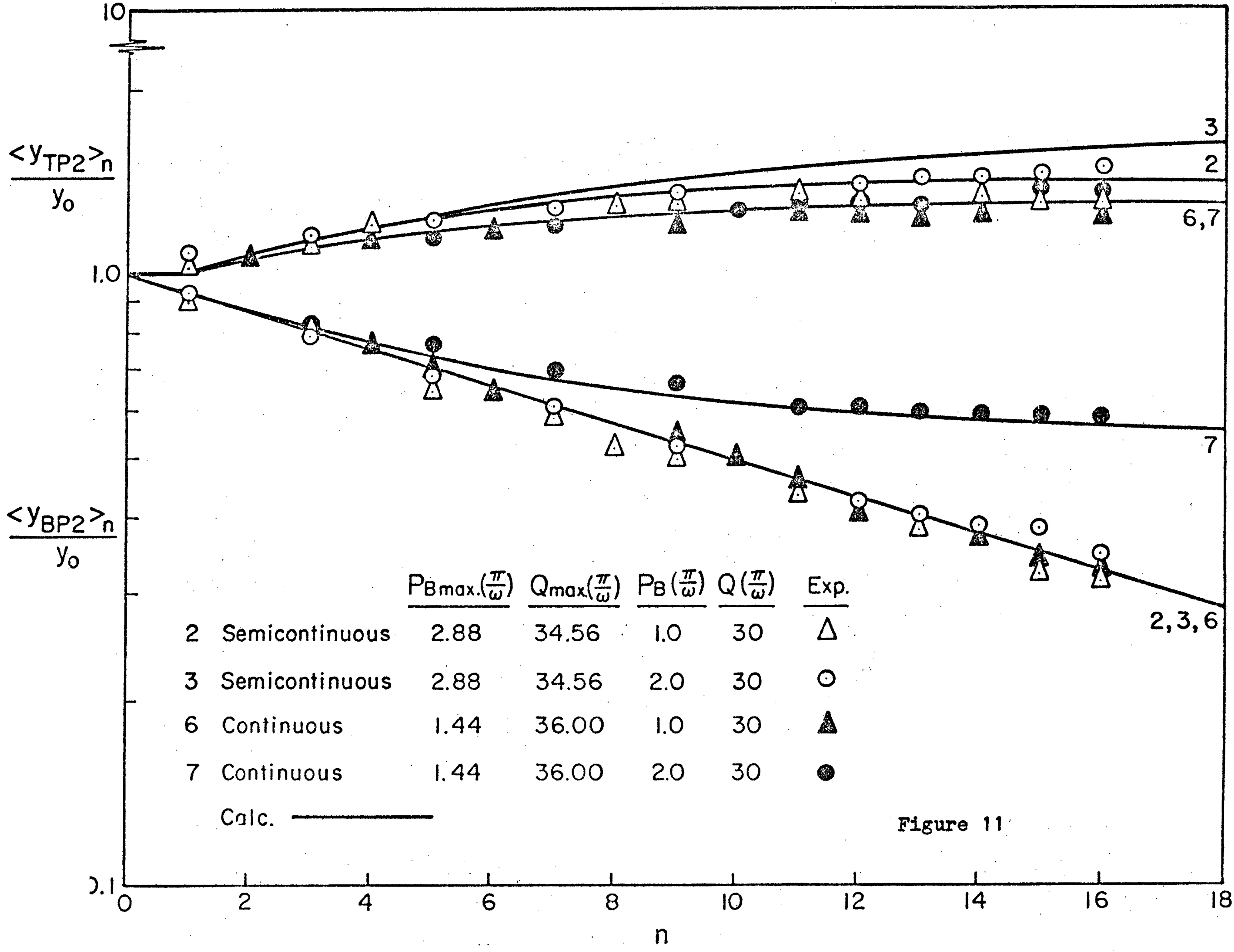
10
1.0
0.1
$\frac{\langle y_{TP2} \rangle_n}{y_o}$
$\frac{\langle y_{BP2} \rangle_n}{y_o}$
0
2
4
6
8
10
12
14
16
18
n
3
2
6,7
7
2,3,6
$P_{B\max}(\frac{\pi}{\omega})$
$Q_{\max}(\frac{\pi}{\omega})$
$P_B(\frac{\pi}{\omega})$
$Q(\frac{\pi}{\omega})$
Exp.
2 Semicontinuous 2.88 34.56 1.0 30 △
3 Semicontinuous 2.88 34.56 2.0 30 ⊙
6 Continuous 1.44 36.00 1.0 30 ▲
7 Continuous 1.44 36.00 2.0 30 ●
Calc.

Figure 11

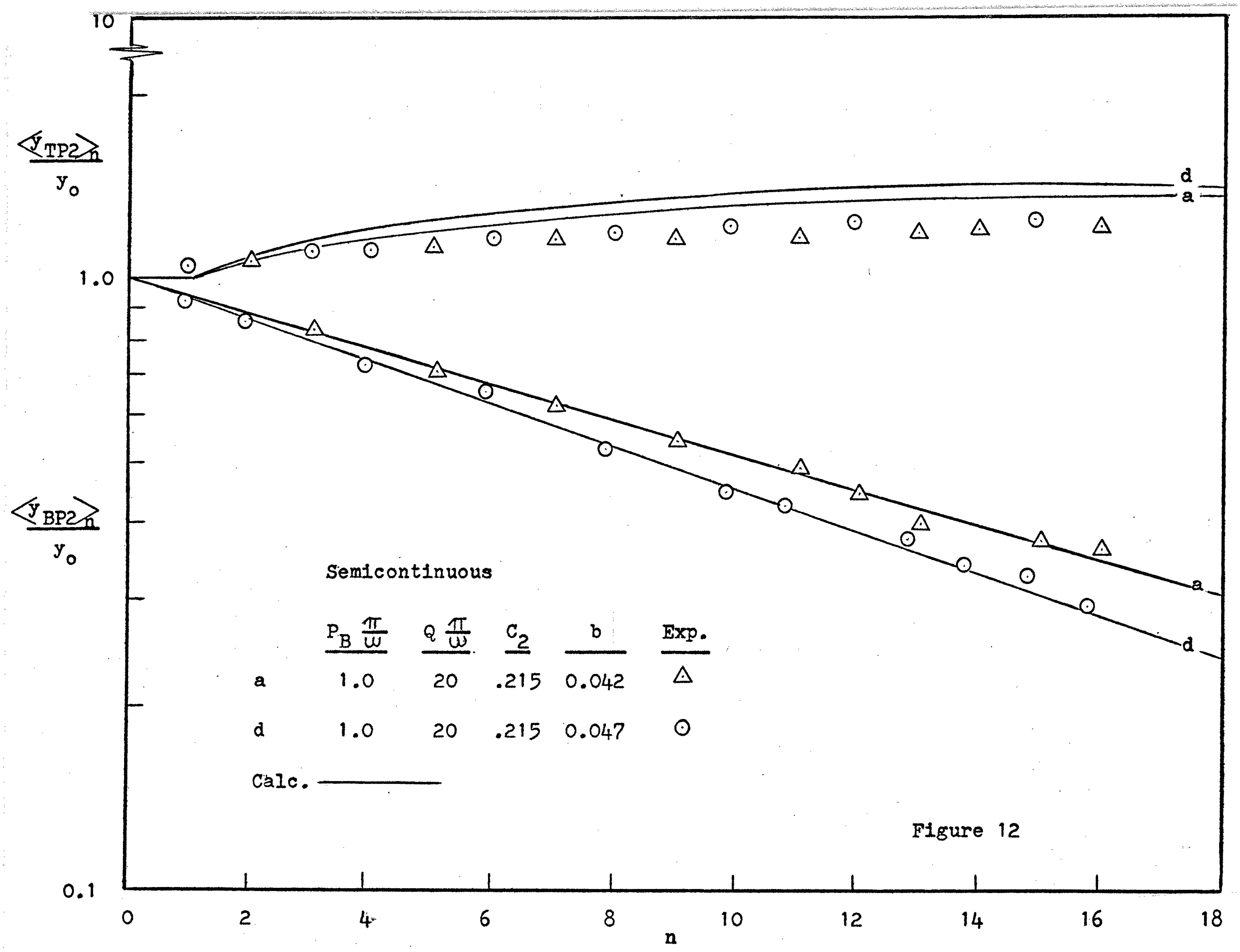

Semicontinuous

	$P_B \frac{\pi}{\omega}$	$Q \frac{\pi}{\omega}$	C_2	b	Exp.
a	1.0	20	.215	0.042	△
d	1.0	20	.215	0.047	⊙

Calc. ———

Figure 12

APPENDIX II

A Summary of the Theory of Parametric Pumping as Compiled for Reference with Regard to Developments in this Paper

A. Development and Solution of the Equation of Transport

The equation of continuity for the mass transport of substance A in a fluid having a constant density and mass diffusivity, considering transport in the z-direction only is:

$$\frac{\partial C_A}{\partial t} + v_z \frac{\partial C_A}{\partial Z} = D_A \frac{\partial^2 C_A}{\partial Z^2} \qquad \text{(A-1)}$$

rate of accumulation of A	+	rate of transport by bulk flow	=	rate of transport by axial diffusion

Since both solid and liquid phases are present, let ϵ be the fraction of volume occupied by the liquid, and let $\partial C_{Af}/\partial t$ and $\partial C_{As}/\partial t$ be the rate of accumulation of A in the liquid and solid phases respectively.
Eq. (A-1) then becomes,

$$(1-\epsilon)\frac{\partial C_{As}}{\partial t} + \epsilon\frac{\partial C_{Af}}{\partial t} + \epsilon v_z \frac{\partial C_{Af}}{\partial Z} = D_A \frac{\partial^2 C_{Af}}{\partial Z^2} \qquad \text{(A-1a)}$$

Define an x and y such that $x = C_{As}/\rho_s$ and $y = C_{Af}/\rho_f$, and assume that the axial diffusion term is a negligible quantity so that

$$(1-\epsilon)\frac{\partial(x\rho_s)}{\partial t} + \epsilon\frac{\partial(y\rho_f)}{\partial t} + \epsilon v_z\frac{\partial(y\rho_f)}{\partial Z} = 0 \qquad \text{(A-1b)}$$

and since all densities are constant,

$$(1-\epsilon)\rho_s\frac{\partial x}{\partial t} + \epsilon\rho_f\frac{\partial y}{\partial t} + \epsilon v_z\, f\frac{\partial y}{\partial Z} = 0 \qquad \text{(A-1c)}$$

(For the definitions and units of the above variables, see Nomenclature, pg. 33). If the equilibrium relationship between the two phases is assumed to be linear,

$$x = M(T)y \qquad \text{(A-2)}$$

where M is the equilibrium constant and is a function of temperature only. Taking the derivative of eq. (A-2) with respect to time gives,

$$\frac{\partial x}{\partial t} = M\frac{\partial y}{\partial t} + y\frac{\partial M}{\partial T}\,\frac{\partial T}{\partial t} \qquad \text{(A-2a)}$$

substituting eq. (A-2a) into eq. (A-1c) and rearranging,

$$\frac{\partial y}{\partial t} + \frac{(1-\epsilon)\rho_s M}{\epsilon\rho_f}\,\frac{\partial y}{\partial t} + \frac{(1-\epsilon)\rho_s}{\epsilon\rho_f}\,y\,\frac{dM}{dT}\,\frac{\partial T}{\partial t} + v_z\frac{\partial y}{\partial Z} = 0 \qquad \text{(A-3)}$$

Let $m = (1-\epsilon)\rho_s M/\epsilon\rho_f$ and rearrange:

$$(m+1)\frac{\partial y}{\partial t} + v\frac{\partial y}{\partial Z} = -\frac{dm}{dT}\frac{\partial T}{\partial t}y \qquad \text{(A-3a)}$$

This hyperbolic partial differential equation will be solved by the method of characteristics as follows:

$$y = f(Z,t) \qquad \text{(A-4)}$$

$$dy = \frac{\partial y}{\partial Z}dZ + \frac{\partial y}{\partial t}dt \qquad \text{(A-4a)}$$

Create arbitrary parameters s and r, so that $Z = Z(s,r)$ and $t = t(s,r)$. Therefore,

$$y = y(s,r) \qquad \text{(A-4b)}$$

and, if r is held constant,

$$\left(\frac{\partial y}{\partial s}\right)_r = \frac{\partial y}{\partial Z}\left(\frac{\partial Z}{\partial s}\right)_r + \frac{\partial y}{\partial t}\left(\frac{\partial t}{\partial s}\right)_r \qquad \text{(A-4c)}$$

Comparing eq. (A-3a) with eq. (A-4c) it is seen that,

$$v = \left(\frac{\partial Z}{\partial s}\right)_r \qquad \text{(A-5)}$$

$$1 + m = \left(\frac{\partial t}{\partial s}\right)_r \tag{A-5a}$$

and

$$-\frac{dm}{dT}\frac{T}{t}y = \left(\frac{\partial y}{\partial s}\right)_r \tag{A-5b}$$

Keeping r constant and rearranging,

$$ds = \frac{dZ}{v} \tag{A-5c}$$

$$ds = \frac{dt}{1 + m} \tag{A-5d}$$

$$ds = \frac{dy}{-\frac{dm}{dT}\frac{\partial T}{\partial t}y} \tag{A-5e}$$

Eliminating ds,

$$\frac{dz}{v} = \frac{dt}{1 + m} = -\frac{dy}{\frac{dm}{dT}\frac{\partial T}{\partial t}y} \tag{A-6}$$

If m is assumed to be a linear function of temperature, a plot like that of figure A-1 will result, where m_h and m_c are constants, proportional to the equilibrium constants, corresponding to hot and cold temperatures T_h and T_c

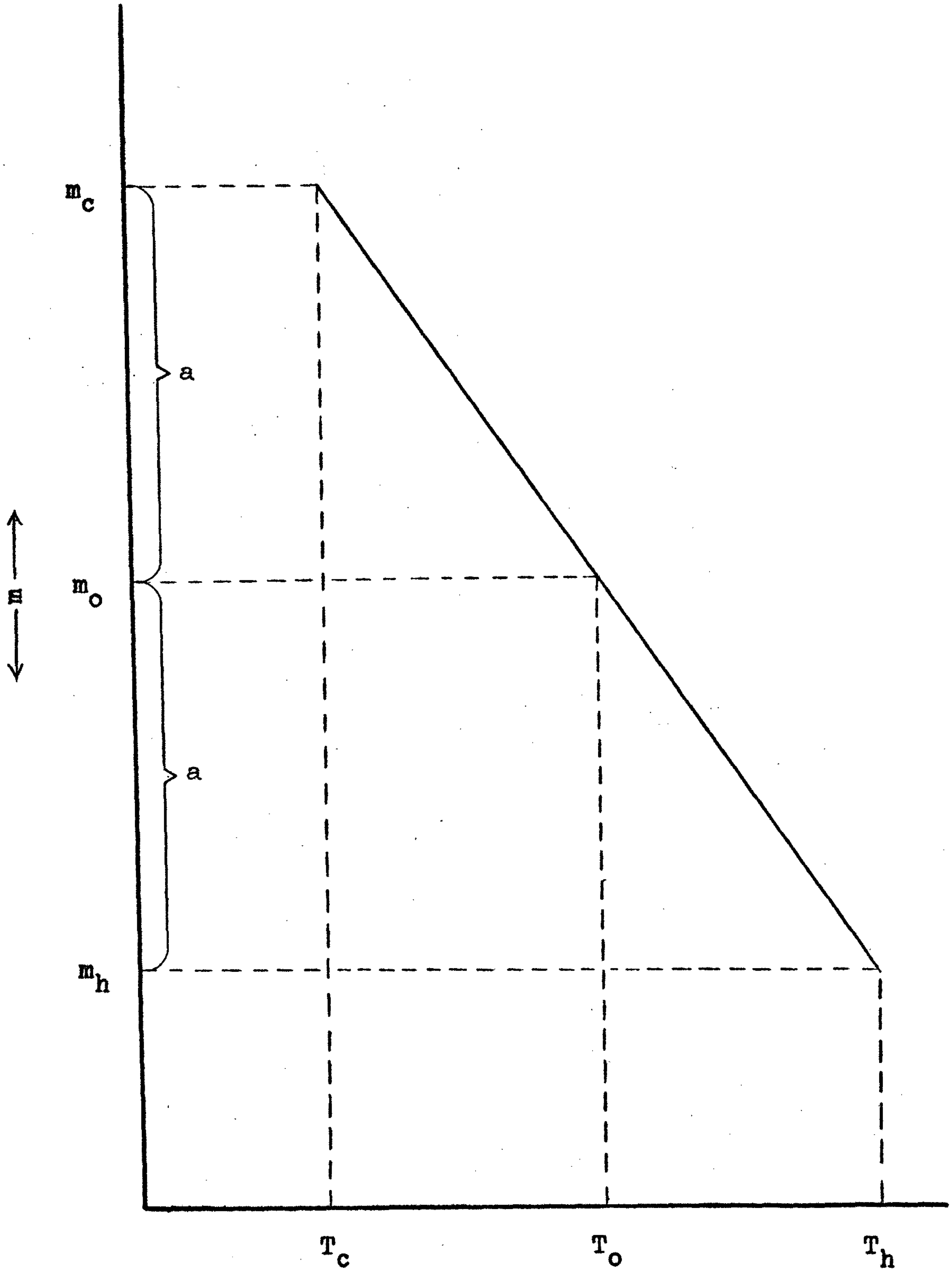

Figure A-1 — The Equilibrium Parameter m as a Linear Function of Temperature respectively, and m_o is a constant midway between m_h and m_c corresponding to the mean temperature T_o. If 'a' is the absolute value of the difference between m_o and m_c or m_h,

$$m_c = m_o + a$$

$$m_h = m_o - a$$

Solving the first part of eq. (A-6) at $T = T_h$ (corresponding to upflow half cycle of parametric pump operation),

$$\frac{dz}{dt} = \frac{v}{1 + m_h} = \frac{v}{1 + m_o - a} \tag{A-6a}$$

Dividing top and bottom by $1 + m_o$,

$$\frac{dz}{dt} = \frac{\dfrac{v}{1 + m_o}}{1 - \dfrac{a}{1 + m_o}} \tag{A-6b}$$

The quantity $a/(1 + m_o)$ is interpreted as a measure of the extent of movement of solute A between solid and liquid phases as a result of temperature change, and is identified by the letter b. Eq. (A-6b) thus becomes,

$$\frac{dz}{dt} = \frac{v}{(1 + m_o)(1 - b)} \tag{A-6c}$$

Similarly, at $T = T_c$ (downflow), the equation becomes

$$\frac{dz}{dt} = \frac{-v}{(1 + m_o)(1 + b)} \tag{A-6d}$$

where the minus sign refers to the downflow direction. Solving the second part of eq. (A-6),

$$\frac{dt}{1 + m} = \frac{-dy}{\frac{dm}{dt}\,y} \tag{A-6e}$$

leading to

$$\int_{m_c}^{m_h} \frac{dm}{1 + m} = - \int_{y_c}^{y_h} \frac{dy}{y} \tag{A-6f}$$

yielding

$$\ln\frac{1 + m_c}{1 + m_h} = \ln\frac{1 + m_o + a}{1 + m_o - a} = \ln\frac{1 + \frac{a}{1 + m_o}}{1 - \frac{a}{1 + m_o}}$$

$$= \ln\frac{1 + b}{1 - b} = -\ln\frac{y_c}{y_h}$$

or

$$\frac{y_h}{y_c} = \frac{1 + b}{1 - b} \tag{A-6g}$$

Eq. (A-6g) shows that the concentration of solution during the hot half cycle differs from that of the cold half cycle by a factor of (1 + b)/(1 - b).

A summary of the assumptions made in developing these equations follows:

1) Instantaneous equilibrium between the adsorbate in the solid and liquid phases

2) Instantaneous temperature changes

3) Fluid with constant density

4) A linear model of equilibrium adsorbtion

5) A linear dependence of the equilibrium constant on temperature

6) One dimensional flow with no axial diffusion

7) Plug flow

B. Characteristic Lines

Eq. (A-6c) corresponds to the motion that a particular wave of constant concentration possesses when moving up the column at a constant rate, which is proportional to the interstitial velocity v and the nature of the equilibrium parameter b. Eq. (A-6d) similarly corresponds to the motion of the concentration front when moving down the column at a constant rate, which is less than the upward rate for the same value of v. Thus, if the distance of penetration z of the wave front is plotted against the time, a line having a slope equal to $v/(1 + m_o)(1 - b)$ during the hot half cycle and $v/(1 + m_o)(1 + b)$ during the cold half cycle will result. Figure B-1 shows such a plot extended over three cycles. Each "zig-zag" line represents the position of a particular concentration front at a particular time. Note that the concentration of such a front is $(1 - b)/(1 + b)$ times the hot half cycle concentration during the cold half cycle.

It is seen from figure B-2 that a material balance around the feed point of the continuous pump gives an upward rate of fluid inside the column equal to $Q(1 - \phi_B)$ and a downward rate equal to $Q(1 + \phi_B)$. Since the interstitial velocity of column fluid is equal to the volumetric rate divided by the fluid area ϵA, it follows that the upward velocity of fluid in the continuous pump is given by

$$v_1 = \frac{Q(1 - \phi_B)}{A\epsilon} \qquad \text{(B-1)}$$

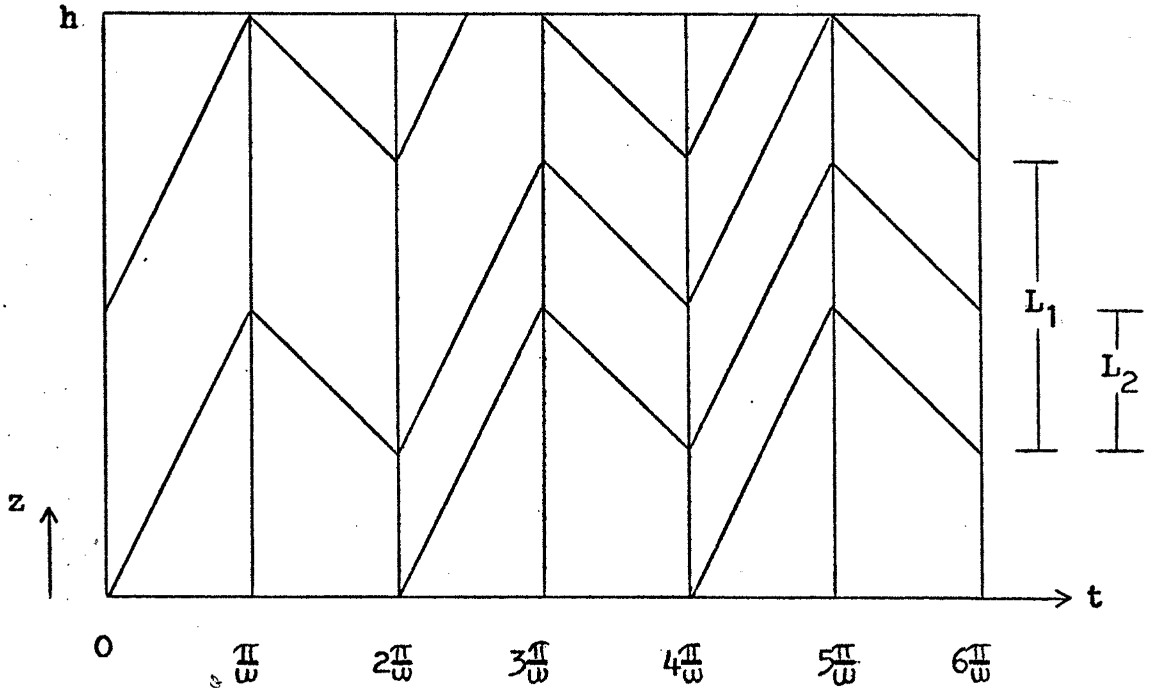

Figure B-1 — Concentration Front Characteristics for Region One

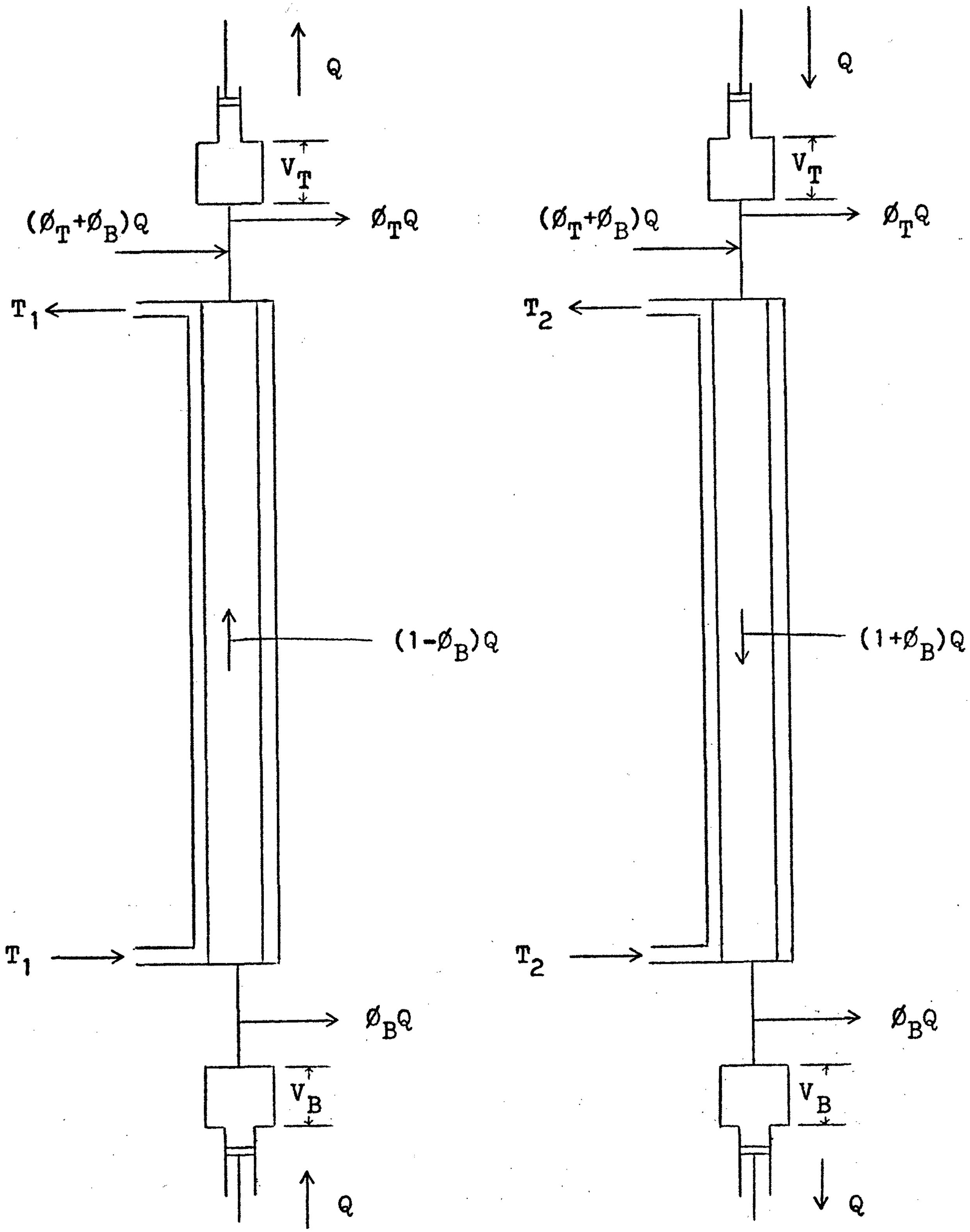

Figure B-2 — The Continuous Parametric Pump and the downward velocity is

$$v_2 = \frac{Q(1 + \phi_B)}{A\epsilon} \qquad \text{(B-1a)}$$

If these velocities are substituted into eqs. (A-6c) and (A-6d) for upflow and downflow respectively, the following equations result:

$$\frac{dz}{dt} = \frac{Q(1 - \phi_B)}{A\epsilon(1 + m_o)(1 - b)} \qquad \text{(B-2)}$$

for upflow

and

$$\frac{dz}{dt} = \frac{Q(1 + \phi_B)}{A\epsilon(1 + m_o)(1 + b)} \qquad \text{(B-2a)}$$

for downflow

Integrating eqs. (B-2) and (B-2a) between the half cycle time limits 0 and π/ω, will yield equations for the penetration distance of a particular wave front during upflow and downflow, identified by L_1 and L_2 respectively, or, for the continuous pump,

$$L_1 = \frac{Q(1 - \phi_B)}{A\epsilon(1 + m_o)(1 - b)} \frac{\pi}{\omega} \qquad \text{(B-2b)}$$

and

$$L_2 = \frac{Q(1 + \phi_B)}{A\epsilon(1 + m_o)(1 + b)} \frac{\pi}{\omega} \qquad \text{(B-2c)}$$

From figure B-3 it is seen that a similar material balance for the semicontinuous pump gives upward and downward fluid rates of Q and $Q(1 + \phi_B)$ respectively, so that

$$v_1 = \frac{Q}{A\epsilon} \qquad \text{(B-3)}$$

and

$$v_2 = \frac{Q(1 + \phi_B)}{A\epsilon} \qquad \text{(B-3a)}$$

which lead to the penetration distance equations for the semicontinuous pump, given by

$$L_1 = \frac{Q}{A\epsilon(1 + m_o)(1 - b)} \frac{\pi}{\omega} \qquad \text{(B-3b)}$$

$$L_2 = \frac{Q(1 + \phi_B)}{A\epsilon(1 + m_o)(1 + b)} \frac{\pi}{\omega} \qquad \text{(B-3c)}$$

Note that the expression for L_2 is the same for both types of pumping.

For either kind of pump, depending upon the sizes of L_1 and L_2 in relation to themselves and the height of the column h, three distinct patterns of the distribution of concentration fronts entering and leaving the column exist. As a result, the steady state concentrations of top and bottom product may be quite different for pumps

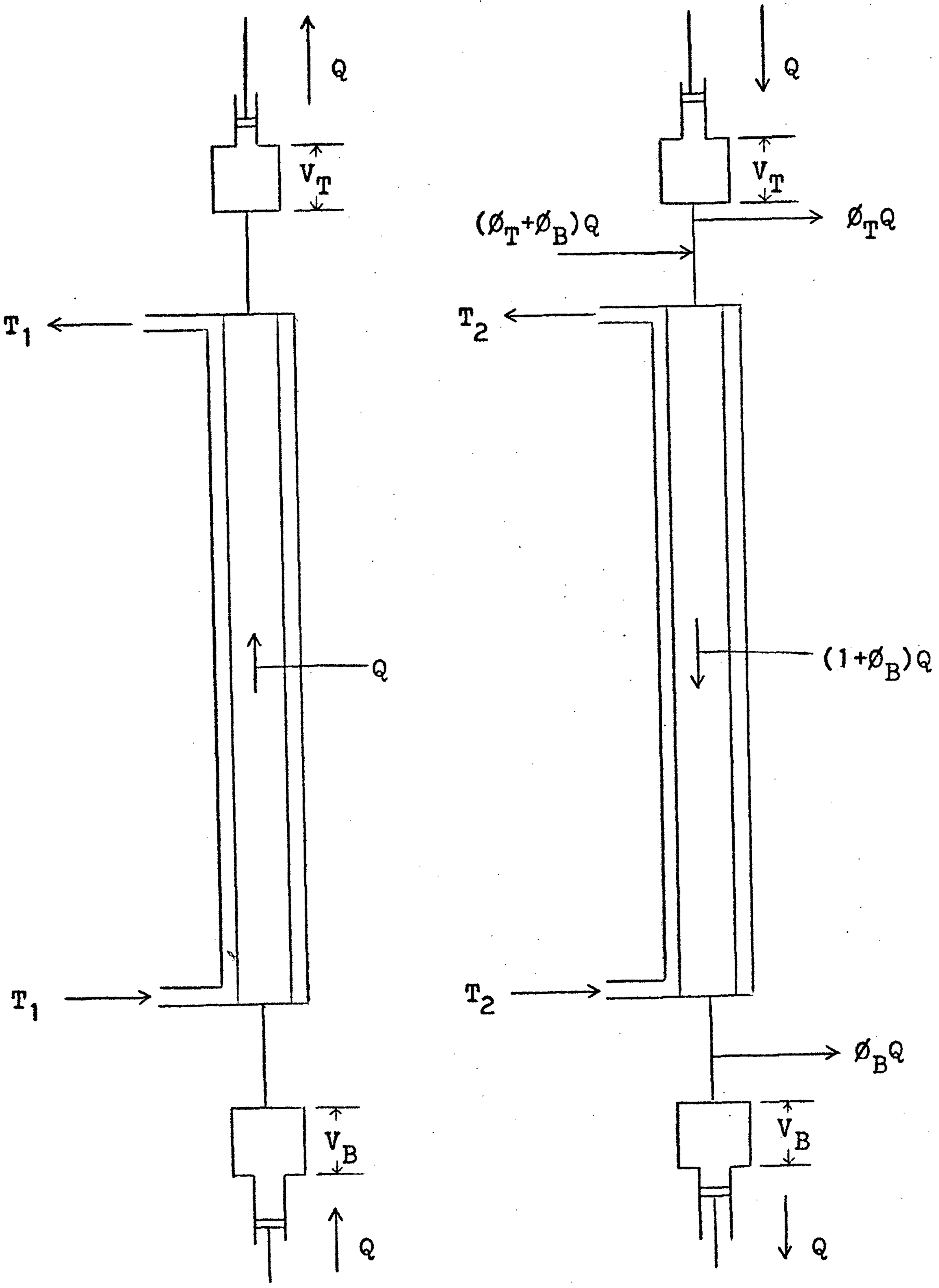

Figure B-3 — The Semicontinuous Parametric Pump operating with dissimilar patterns. Figure B-4 shows three regions of operation, each characterized by different steady state concentration patterns. When a pump is operated in region one ($L_2 \leqslant L_1$ and h) the steady state concentration of solute will be zero. Operation in either of the other two regions, however, will result in only partial removal of solute at steady state.

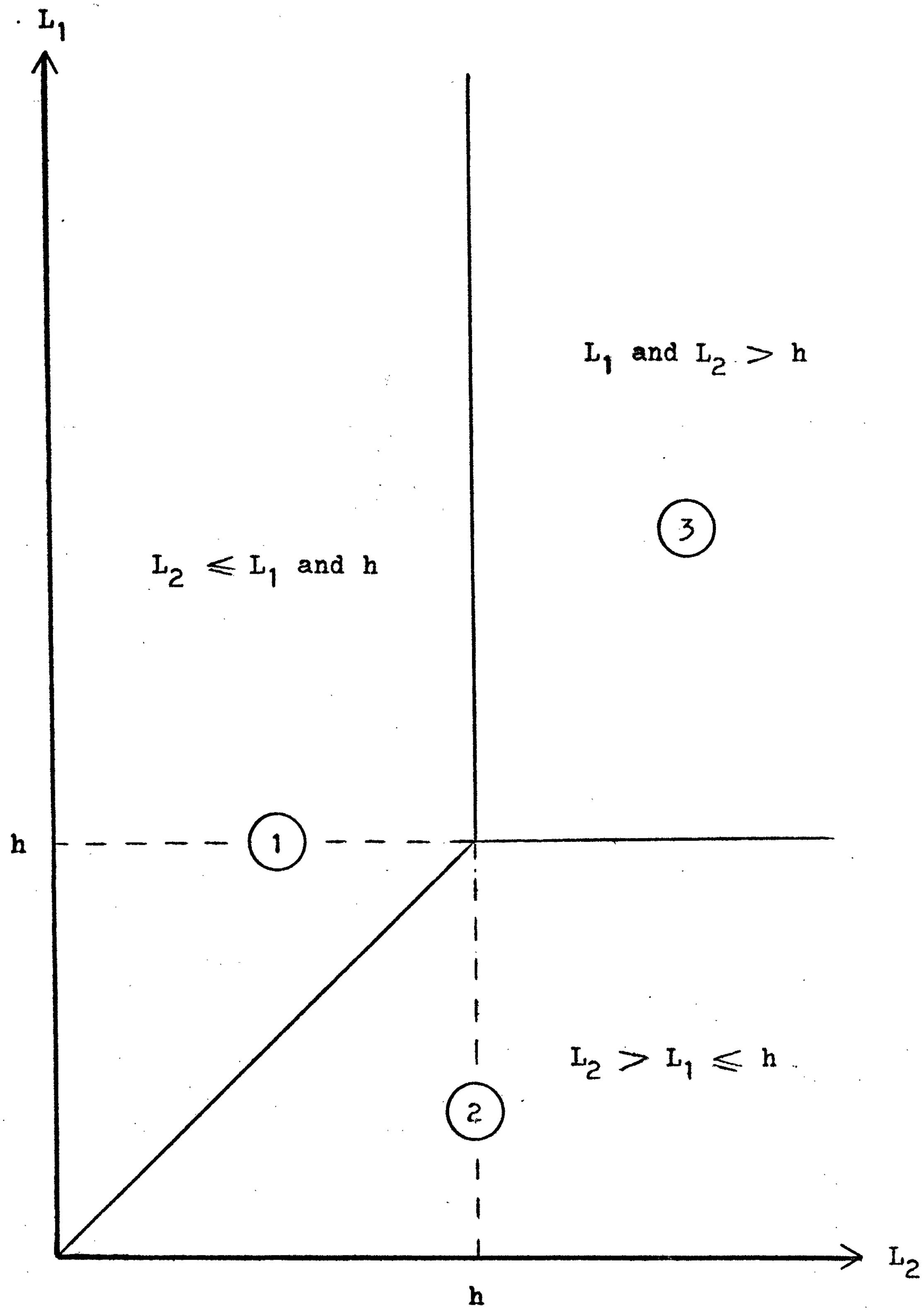

Figure B-4 — The Three Regions of Parametric Pump Operation

C. Determination of Top and Bottom Product Transient Concentrations and the Value of b

For a given pump operating in a given region, two types of equations may be developed — internal equations and external equations. An internal equation involves a solute material balance on material entering or leaving the column taking into account the types and amounts of concentration fronts involved. An external equation is a solute material balance on streams flowing to and from a reservoir considering the presence of any adjacent feed and product streams, taking into account the dead volume of the reservoirs. Since an external and an internal equation may be written for both the bottom and top of the column, a total of four equations solved simultaniously will yield the transient solution for the top and bottom concentrations for that particular region of operation. Such equations for all three regions for both types of pumps may then be solved on a computer using certain experimental parameters for data.

The equation for the average bottom product concentration collected during the downflow cycles of both semicontinuous and continuous pumps is

$$\langle y_{BP2} \rangle_n = y_o \left(\frac{1 - b}{1 + b} \right) \left(\frac{\frac{1 - b}{1 + b} + C_2}{1 + C_2} \right)^{n - 1} \quad n \geqslant 1 \qquad \text{(C-1)}$$

Let A be the term which is taken to the n − 1 power and divide by y_o so that

$$\frac{\langle y_{BP2} \rangle_n}{y_o} = \left(\frac{1-b}{1+b}\right) A^{n-1} \qquad \text{(C-1a)}$$

Taking the log of both sides and rearranging,

$$\frac{\log \dfrac{\langle y_{BP2} \rangle_n}{y_o} - \log\left(\dfrac{1-b}{1+b}\right)}{n-1} = \log(A)$$

(C-1b)

The left side of eq. (C-1b) is seen as the slope of $\log(\langle y_{BP2} \rangle_n / y_o)$ vs. n, which will be designated as α. Note, $\log((1-b)/(1+b)) = \log(y_o(1-b)/y_o(1+b))$

$= \log(\langle y_{BP2} \rangle_n / y_o)$ (see eq. (A-6g))

Therefore,

$$10^{\alpha} = A = \frac{\dfrac{1-b}{1+b} + C_2}{1 + C_2} = \frac{1 - b + C_2(1+b)}{1 + b + C_2(1+b)} = \frac{1 - b + C_2(1+b)}{b + C_2 b + 1 + C_2}$$

(C-1c)

Solving for b,

$$b = \frac{1 - 10^{\alpha} + C_2(1 - 10^{\alpha})}{1 + 10^{\alpha} - C_2(1 - 10^{\alpha})} \qquad \text{(C-1d)}$$

Hence, if bottom product is collected for n cycles and the concentration is measured by experimental means, a plot of $\langle y_{BP2} \rangle_n / y_o$ vs. n on semilog paper for finding α, and knowledge of the bottom reservoir dead volume is all that is needed for the determination of b.